THE EFFECT OF URBAN AIR QUALITY ON VISIBILITY

PHASE I: COMPREHENSIVE RESEARCH AND MONITORING PROTOCOL

RESEARCH MANAGEMENT Division

Alberta Environment

89-00366/

For information on reports published by the Research Management Division, contact:

Alberta Environment Library
14th Floor, Oxbridge Place
9820 - 106 Street
Edmonton, Alberta
T5K 2J6

(403) 427-5870

This report may be cited as:

Barlow, F., L. Cheng, E. Peake, A. Davis, and M. English. 1987. The effect of urban air quality on visibility - Phase I: comprehensive research and monitoring protocol. Prep. for Research Management Division, Alberta Environment by Atmospheric Sciences Department, Alberta Research Council and Kananaskis Centre for Environmental Research, University of Calgary. RMD Report L-103. 81 pp.

THE EFFECT OF URBAN AIR QUALITY ON VISIBILITY

PHASE I: COMPREHENSIVE RESEARCH AND MONITORING PROTOCOL

by

F. BARLOW
L. CHENG
E. PEAKE[1]
A. DAVIS
M. ENGLISH

Atmospheric Sciences Department
Alberta Research Council

[1]Kananaskis Centre for Environmental Research
University of Calgary

for

RESEARCH MANAGEMENT DIVISION

Alberta Environment

RMD Report L-103

1988

EXECUTIVE SUMMARY

The results of Phase I of a research program designed to study the effect of urban air quality on visibility in the Calgary region are presented. Included in the results are an experimental design for a full assessment program, instrumentation development, aerosol profile analysis and field measurements. A proposed Phase II of the project would focus on implementation of the plan.

The objectives of Phase I were the following:

1) To develop and design a detailed comprehensive research and monitoring protocol.

2) To design, construct, install and test instrumentation and analytical procedures required for the successful implementation of the protocol designed in (1).

3) To show the usefulness of measurements made with an appropriately instrumented research aircraft through an analysis of selected aerosol data previously collected by the Alberta Research Council in central Alberta and to provide preliminary information on the vertical profile of atmospheric pollutants in the Calgary region.

4) To develop computer procedures for radiation modelling to complement the measurement program proposed in (1).

For the first objective, a detailed experimental design for a comprehensive Phase II project is presented. The plan includes a climatological study of visibility, a surface measurement program, and an aircraft measurement program. A two-year operational period is proposed.

Phase I results include the development of the Kananaskis Atmospheric Pollution Sampler (KAPS)-impactor sampling system for surface measurement of visibility-reducing pollutants. Field tests of the system and measurements of particulates and gaseous emissions were successfully completed. The tests show that gaseous and particulate pollutants can be separated and particulate aerosols size fractionated.

The use of aircraft measurements of aerosols to determine light extinction coefficients over urban areas was tested. Vertical profiles of aerosol concentration were derived from data previously collected by the Intera-Alberta Research Council research aircraft. Illustrative case studies of "urban" and "rural" aerosol profiles are given for the Calgary region. These profiles indicate that significant differences can occur between sites and illustrate the valuable contribution a research aircraft can make in air quality studies.

Monitoring of haze using solar radiometric techniques was also tested. An irradiance measurement program initiated near the Calgary International Airport is described and derived aerosol loadings analyzed. Problems with instrument operation are noted and a preferred system using a filterwheel radiometer for "narrow-band" measurements is suggested. These measurements indicate the possibility of using solar radiometric techniques for monitoring regional aerosol loading.

TABLE OF CONTENTS

		Page
LIST OF TABLES		xi
LIST OF FIGURES		xii
ABSTRACT		xv
ACKNOWLEDGMENT		xvi
1.	INTRODUCTION	1
1.1	Theoretical Background	2
1.2	Project Objectives	4
2.	DEVELOPMENT OF THE KANANASKIS ATMOSPHERIC POLLUTANT SAMPLER	7
2.1	Description of the KAPS-Impactor Sampling System	8
2.2	Instrument Operation and Analysis Procedures	12
2.3	Testing of the KAPS-Impactor System	13
2.4	Conclusions of Chemical Smpling Technique Development	16
3.	ANALYSIS OF AIRCRAFT MEASUREMENTS OF AEROSOL PROFILES	17
3.1	Aircraft Instrumentation and Aerosol Sampling Procedures	17
3.2	Urban Aerosol Profile Case Study (June 22, 1983)	19
3.3	Rural Aerosol Profile Case Study (July 13, 1984)	19
3.4	Comparison of Urban and Rural Profiles	24
3.5	Calculations and Discussion of Aircraft Data Analysis	27
3.6	Conclusions and Discussion of Aircraft Data Analysis	29
4.	IRRADIANCE MEASUREMENT PROGRAM AND AEROSOL TURBIDITY	32
4.1	Aerosol Optical Depth	32
4.2	Radiation Model	34
4.3	Model of Spectral Aerosol Optical Depth	36
4.4	Radiation Measurement Program	37
4.5	Spectral Measurement Program	40
4.6	Results of Radiation Measurement Program	41
4.6.1	Field Measurements of Irradiance Components	41
4.6.2	Comparison of Direct Beam Measurements	46
4.6.3	Calculated Aerosol Optical Depths	48
4.6.4	Radiative Responses to Aerosol Optical Depths	50
4.6.5	Aerosol Optical Depths and Meteorological Conditions	51
4.6.6	Spectral Measurement Results	53
4.7	Summary and Conclusions of Radiation Measurement Program	55

Continued . . .

TABLE OF CONTENTS (CONCLUDED)

		Page
5.	PROPOSED EXPERIMENTAL DESIGN FOR PHASE 2	57
5.1	Climatological Study of Visibility in the Calgary Region ...	58
5.2	Surface Measurement Program	59
5.2.1	Gaseous Measurements	61
5.2.2	Aerosol Measurements	63
5.2.3	Extinction Coefficient Measurements	64
5.2.4	Meteorological Measurements	64
5.2.5	Solar Radiation Measurements	64
5.3	Aircraft Measurement Program	65
5.4	Expected Results	67
5.5	Conclusions	68
6.	SUMMARY AND CONCLUSIONS	69
7.	REFERENCES	70
8.	APPENDIX	73

LIST OF TABLES

		Page
Table 1.	X-Ray Fluorescence of Air Filters. List of Elements and Detection Limits.....	14
Table 2.	Results of Field Test of KAPS-Impactor Sampling System.....	15
Table 3.	Spectral Bands Determined by Schott Optical Filters for Determination of Narrow Band Aerosol Optical Depths.....	41
Table 4.	Phase II surface site and aircraft measurements.....	62

LIST OF FIGURES

		Page
Figure 1.	Schematic Diagram of KAPS-Impactor Sampling System..	9
Figure 2.	Aerosol Particle Concentration Profile for Calgary, 22 June 1983.....	20
Figure 3.	The Relative Humidity and Equivalent Potential Temperature Profiles for Calgary, 22 June 1983.....	21
Figure 4.	Aerosol Particle Concentration Profile for Red Deer Industrial Airport, 13 July 1984.....	22
Figure 5.	The Relative Humidity and Equivalent Potential Temperature Profiles for Red Deer Industrial Airport, 13 July 1984.....	23
Figure 6.	Aerosol Particle Concentration Spectra for Three Levels, 770 mb, 850 mb and Ground Level for Calgary, 22 June 1983.....	25
Figure 7.	Aerosol Particle Concentration Spectra for Three Levels, 770 mb, 850 mb and Ground Level for Red Deer Industrial Airport, 13 July 1984.....	26
Figure 8.	Extinction Efficiency versus Size Parameter for Ammonium Sulphate, Ammonium Bisulphate and Sulphuric Acid Spheres Using a Visible Light Wavelength of 0.55 μm.....	28
Figure 9.	Particle Extinction Coefficient Profiles (Visible Wavelength 0.55 μm) for Calgary, 22 June 1983.....	30
Figure 10.	Particle Extinction Coefficient Profiles (Visible Wavelength 0.55 μm) for Red Deer Industrial Airport, 13 July, 1984.....	31
Figure 11.	Solar and Net Radiation For March 8, 1986 (One-Minute Averages). Broken Cloud Conditions.....	42
Figure 12.	Solar and Net Radiation for March 9, 1986 (One-Minute Averages). Overcast Cloud Conditions....	43
Figure 13.	Solar Radiation Direct and Diffuse Components for April 7, 1986 (One-Minute Averages).....	44
Figure 14.	Comparison of Pyrheliometer Measured and Residually Derived Direct Beam Irradiance Values (n=286).....	47
Figure 15.	Calculated Hourly Aerosol Optical Depths (τ_a) for April 7, 1986.....	49

Continued . . .

LIST OF FIGURES (CONCLUDED)

		Page
Figure 16.	Radiative Response to Aerosol Optical Depths for April 7, 1986	52
Figure 17.	Measured Spectral Aerosol Optical Depths for April 9, 1986	54
Figure 18.	Map of City of Calgary Showing Location of Proposed Observation Sites	60
Figure 19.	Typical Flight Path for Aircraft Measurement Program	66
Figure A.1.	Measured Solar Radiation Components for March 1 to 5, 1986 (Calgary)	75
Figure A.2.	Measured Solar Radiation Components for March 6 to 10, 1986 (Calgary)	76
Figure A.3.	Measured Solar Radiation Components for March 11 to 15, 1986 (Calgary)	77
Figure A.4.	Measured Solar Radiation Components for March 16 to 20, 1986 (Calgary)	78
Figure A.5.	Measured Solar Radiation Components for March 21 to 25, 1986 (Calgary)	79
Figure A.6.	Measured Solar Radiation Components for March 26 to 30, 1986 (Calgary)	80
Figure A.7.	Measured Solar Radiation Components for March 31 to April 4, 1986 (Calgary)	81
Figure A.8.	Measured Solar Radiation Components for April 5 to 9, 1986 (Calgary)	82

ABSTRACT

A comprehensive research plan has been developed to study the effect of urban air quality on visibility.

In preparation for implementation of the plan, a number of measurement techniques and analysis procedures have been developed and tested. Specifically, the KAPS-impactor system has been developed to separate particulate and gaseous pollutants with a minimum of alteration in particle composition and with size fractionation of the particulates. As well, analysis procedures have been developed to produce vertical profiles of aerosol concentrations and a numerical model of Mie scattering has been developed to calculate extinction coefficients due to scattering and absorption by aerosols from data collected with a research aircraft. Finally, irradiance instruments have been tested, procedures for calculating aerosol loading have been derived and optical depth have been calculated.

ACKNOWLEDGEMENTS

The authors would like to acknowledge the assistance of Ms. L. Phillips, Mr. J. Mason and Mr. R. Myrick of the Alberta Research Council in setting up and monitoring the radiation instruments and in analyzing data from these instruments. In addition, discussions with Dr. A. Harrison and Dr. C. Coombes of the Department of Physics, University of Calgary were very helpful in the formulation of the comprehensive research plan.

This project was jointly funded by Alberta Environment and the Alberta Research Council.

1. INTRODUCTION

Urban air quality has been identified, in recent public surveys in Alberta, as a leading environmental concern. In urban areas, atmospheric pollution generates secondary pollutants through radiation mediated photochemistry. Reduced visibility is one of the most obvious and unpleasant adverse consequences of urban air pollution. This attenuation of light has a variety of negative effects on the urban dweller: a loss of visual aesthetic quality, a reduction in sunshine intensity and changes in spectral character, interference with aviation activities and even possible inadvertent weather and climate modification. The deterioration of the visual environment can be very pronounced and, in severe cases, can be viewed as a hazy "brown cloud" encompassing the urban area (Wolff et al., 1980). The increasing occurrence of such conditions has been one of the unfortunate side effects accompanying urban development.

This deterioration of visibility is the result of scattering and absorption of incident solar irradiance by a complex atmospheric suspension of gaseous pollutants and aerosols. Particulate aerosols act as optical filters resulting in regional scale haze and reduced visibility. These aerosols are a mixture of natural and anthropogenic particulates, derived from a variety of sources including soil particles, sea salt, ash, volcanic dust, and sulphates and nitrates from photochemical and catalytic oxidation (Paltridge and Platt, 1976). In urban areas, man's activities provide an additional contribution from flyash, industrial source particles, vehicular emissions and photochemically produced particles from gaseous pollutants. Studies of the effects of these atmospheric pollutants on visibility have been conducted in some major world urban areas (Wolff et al., 1980; Groblicki et al., 1981; White and Roberts, 1977; Lyons and Cutten, 1975; Buma, 1960; and, Leaderer et al., 1981).

In Alberta, urban photochemical pollutants have been studied with special reference to meteorological conditions (Sandhu, 1975). Harrison and Mathai (1980) have studied the aerosol size distributions and their relation to visibility in Calgary. Their approach concentrated on the aerosol physical characteristics affecting attenuation. At the same time, Peake (1980) determined the chemical composition of particulate matter and aerosols over Calgary. These studies have indicated that the potential for serious pollution problems exists in both Edmonton and Calgary.

The efficient management of urban air resources and the planning and design of environmental legislation, impact assessments, and land use planning requires a comprehensive air quality assessment. However, the above studies were not coordinated and do not give sufficient information to determine the aerosol formation mechanisms and sources of visibility reduction. Furthermore, because of the unique meteorological and climatological characteristics of Alberta, results from other locations are not directly applicable to central Alberta. Thus further research is required in this area. Because of this need, a project to study the effect of urban air quality on visibility was initiated.

1.1 THEORETICAL BACKGROUND

Urban atmospheric pollutants (gaseous and particulate) affect visibility by the scattering and absorption of incident solar radiation. The brownish discolouration of the atmosphere is primarily due to the scattering and absorption of aerosols. The extent and quality of this effect depends largely on the physical and chemical characteristics of the aerosols. Waggoner and Charlson (1977) studied

the brown haze in Denver and estimated that the discolouration produced by aerosols was at least twice that produced by NO_2. He also determined that approximately one third of the light extinction due to aerosols was from absorption rather than scattering. Groblicki et al., (1981) have shown that the absorption by aerosols was largely due to graphitic carbon.

The attenuation of incident radiation by atmospheric pollutants can be expressed in terms of the the extinction coefficient b_{ext}, which is the sum of the individual contributions:

$$b_{ext} = b_{ap} + b_{ag} + b_{sp} + b_{sw} + b_{sg}, \qquad (1.1)$$

where b_{ap} and b_{ag} are the absorption by particles and gases respectively , b_{sp} and b_{sw} are the scattering from dry particulate matter and by water associated with the particles respectively and b_{sg} is the gaseous Rayleigh scattering which is commonly considered to be constant and insignificant when compared to the other contributors. The relation between visibility V and the extinction coefficient is usually given by the Koschmieder formula:

$$V = 3.9 / b_{ext}. \qquad (1.2)$$

Determination of the various parameters of Equation 1.1 requires either direct measurement using specialized instruments or indirect calculation based upon chemical composition and theoretical considerations. Overall extinction, b_{ext},can be measured using telephotometers over known pathlengths. The scattering characteristics (e.g. b_{sp}) can be directly measured using integrating nephelometers. Concurrent measurements of total extinction and scattering can then provide estimates of the absorption terms by residual techniques.

1.2 PROJECT OBJECTIVES

Because of fiscal restraints, the project was divided into two phases: Phase I was to focus on the development of a comprehensive experiment plan, the results of which would meet the needs of urban air resources management. As part of the plan development, measurement and analysis techniques and procedures required in the implementation of the plan were also to be developed and tested. As well, some specialized instrumentation was to be constructed. Phase II of the project would then focus on implementation of the plan.

This report is the final report for Phase I of the study. In detail, the objectives of Phase I were:

1) To develop and design a detailed comprehensive research and monitoring protocol to:

    a) characterize and quantify the temporal and spatial variability of the chemical and physical characteristics of the urban aerosol loading (gases and particulates);

    b) determine the relationship between visibility degradation and aerosol loading;

    c) identify what sources contribute to the aerosol loading and the relative impact of each source;

    d) assess the effects of aerosols on the radiation and energy budgets of the urban area.

    The monitoring protocol was designed for implementation in the Calgary area.

2) To design, construct, install, and test instrumentation and analytical procedures required for the successful implementation of the protocol designed in (1). This involved:

   a) designing and testing monitoring equipment and analytical procedures for the collection of aerosols and for the analysis of the aerosol's physical and chemical characteristics. As well as establishing a data base for the chemical and physical characteristics of urban aerosols.

   b) setting up a solar irradiance measurement program to develop and test radiometric measurement and modelling procedures for determining atmospheric aerosol loading and concurrent irradiance values (i.e. radiative responses to aerosols);

3) To show the usefulness of measurements made with an appropriately instrumented research aircraft through an analysis of selected aerosol data previously collected by the Alberta Research Council in central Alberta and to provide preliminary information on the vertical profile of atmospheric pollutants in the Calgary region.

4) To develop computer procedures for radiation modelling to complement the measurement program proposed in (1).

Subsequent sections of this report will give the results for these objectives. Section 2 outlines the development and testing of the KAPS-impactor aerosol sampling system for determining the chemical composition and size fractions of pollutants. Section 3 presents the results of the analysis of the aircraft data for urban and rural aerosol profiles. This section also includes a discussion of the development of the aerosol-scattering models and their application to

the two test profiles. The results of the radiation measurement and turbidity program are presented in Section 4. Section 5 of the report presents the suggested experimental design for implementation in Phase II. A summary of the achievements of Phase I is given in Section 6.

2. DEVELOPMENT OF THE KANANASKIS ATMOSPHERIC POLLUTION SAMPLER

This section describes the KAPS-impactor system developed and tested during Phase I of the project. This system meets the requirements of urban aerosol sampling as discussed below. A detailed description of the developed system and its operational procedure is given in this section and the section closes with a presentation of the results of system tests during Phase I.

Although visibility reducing aerosols occur primarily in the 0.1 to 1.0 μm particle diameter range, it is desirable to obtain chemical speciation of all aerosols for the determination of the formation mechanisms. Furthermore it is necessary to chemically characterize the aerosols to determine the species responsible for the visibility reduction. Sulphate, nitrate, ammonium, silicon, and elemental carbon are selected to account for the majority of the visibility reducing fine particle mass. In addition, elements are measured which can serve as tracers of specific particulate emission sources: Al, Si, K, Ca, Ti, V, Mn, Fe, Zn, Br, Ba, Pb, and As. For example, possible tracer assignments include motor vehicles (Pb, Br, Ba), soil (Al, Ca, Si, Ti, Fe), combustion of oil (V), and combustion of coal (As, Al, Ca, Ti, Fe).

The proposed system is designed to provide the required information on visibility reducing aerosols in Calgary. The system consists of the Kananaskis Atmospheric Pollutant Sampler (KAPS) coupled to a particle sizing cascade impactor. Such a system provides the ability to separate and collect particles according to size with a minimum of alteration in particle composition caused by gas-particle reactions. Acid gases such as nitric acid, nitrous acid, and sulphur dioxide as well as ammonia are removed from the sampling stream by annular denuders (Possanzini et al., 1983) prior to collection of the particles. The system will collect particles in 8 size fractions: 5.8-9.0, 4.7-5.8, 3.3-4.7, 2.1-3.3, 1.1-2.1, 0.7-1.1, 0.4-0.7, and 0.0-0.4 μm, when operated at a sampling rate of 28.3 lpm.

It is intended that the KAPS-impactor sampling system be used at a central site during the future measurement program. Although it would be desirable to have the system at all sites, fiscal restraints will probably preclude this possibility. Thus at the other sites, aerosols would be collected using a KAPS system attached to a dichotomous sampler. This will allow the separation and collection of fine and coarse particle fractions whose chemical composition has not been significantly changed by fast-particle reactions during sampling. A Teflon virtual impactor would be used as a preseparator at the inlet to remove particles greater than 10 μm in size, which are mainly derived from wind blown soil and which reflect the composition of crustal material. The size range of the coarse fraction would be 2.5 to 10 μm and of the fine fraction, 0-2.5 μm. The exposed filters would be analyzed by x-ray fluorescence spectrometry and the results would be used in source apportionment studies. Three additional KAPS-dichotomous units would be available to provide further areal resolution as necessary.

2.1 DESCRIPTION OF THE KAPS-IMPACTOR SAMPLING SYSTEM

The design of the modified KAPS-impactor system is shown in Figure 1. Ambient air is drawn through the inlet (A) into the preseparator (B). The preseparator is a virtual impactor designed to remove large particles, greater than 10 μm in size, which consist mainly of crustal material from wind blown dust. It prevents significant errors which can be caused by particle bounce and re-entrainment.

The preseparator has a 0.53" diameter inlet orifice and three outlet tubes. The outlet tubes are 1.0" above the impaction surface. This design results in very low turbulence and allows collection of several grams of particulate without overloading the preseparator. Construction material is Teflon allowing passage of nitric acid which would react with metal surfaces.

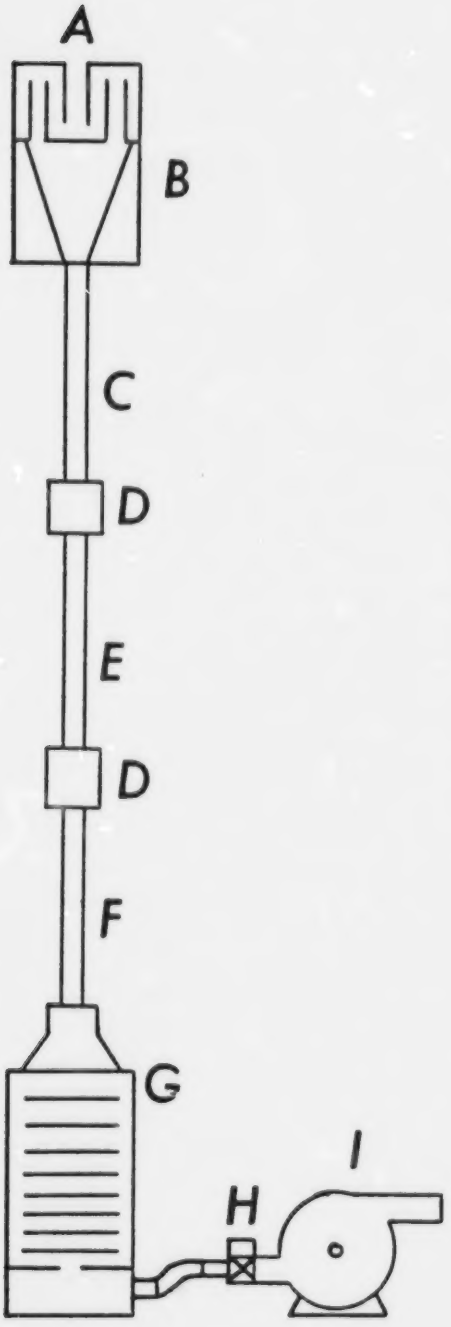

Figure 1. Schematic Diagram of KAPS-Impactor Sampling System.

The air passes through a series of three annular denuder tubes to remove reactive gases. The air, free of reactive gases, enters a modified cascade impactor (G) which separates and collects particles in eight size fractions: 5.9-9.0, 4.7-5.8, 3.3-4.7, 2.1-3.3, 1.1-2.1, 0.7-1.1, 0.4-0.7, and 0.0-0.4 μm. Each annular denuder tube consists of an outer glass tube, three-quarter of an inch outside diameter and 13.20 mm inside diameter, and an inner tube of 10.00 mm outside diameter. The tubes (C, E, and F) and the Teflon connectors (D) are designed to provide laminar flow characteristics preventing particle deposition. (Higher capacity tubes of 30.00 mm inside diameter and appropriate connectors are presently under construction). The annulus walls of the first denuder tube (C) are coated with a sodium carbonate-glycerol mixture and retain nitric acid, nitrous acid, sulphur dioxide, and other acid gases. These gases are major acid species in the atmosphere and react with or are in equilibrium with visibility reducing aerosols. Tube C also retains some nitrous oxide (about 5% of the atmospheric concentration) which interferes with the measurement of nitrous acid. The second tube (E) retains 5% of the remaining nitrous oxide and is used to correct the nitrous acid value obtained from tube C. The third tube (F) is coated with citric acid and is used to collect ammonia. This system has been tested extensively in both laboratory and field trials and has proven effective for the collection of acid and basic gases. Some particles may also be deposited in the denuder tubes but deposition is negligible when laminar flow is maintained during sampling.

The sampler comprises of eight aluminium stages that are held together by three spring clamps gasketed with O-ring seals. Each impactor stage contains multiple precision drilled orifices. When air is drawn through the sampler, multiple jets of air in each stage direct any airborne particles toward the surface of the collection plate for that stage. The size of the jets is constant for each stage, but is smaller in each succeeding stage. Whether a particle is impacted on any given stage depends on its aerodynamic dimension. The range of particle sizes collected on each stage depends on the jet

velocity of the stage and the cutoff of the previous stage. Any particle not collected on the first stage follows the air streams around the edge of the plate to the next stage where it is either impacted or passed on to the succeeding stage, and so on, until the jet velocity is sufficient for impaction.

Stages 0 and 1 have integral air inlet sections that contain 96 orifices arranged in a radial pattern. Stages 2 through 6 have integral air inlet sections that contain 400 orifices arranged in a circular pattern. The orifices are progressively smaller from top to bottom stages, ranging from 0.1004" diameter on stage 0 to 0.0100" diameter on stage 7. Each stage has a removable stainless steel (3.25" diameter) collection plate. The exhaust section of each stage is approximately 0.75" larger in diameter than the collection plate, allowing unimpacted particles to go around the plate and into the next stage. The top two stainless steel collection plates have 7/8" holes in the centre to allow air flow through the centre also.

Flow of ambient air through the entire KAPS-impactor system is provided by a vacuum pump with an adjustable limiting orifice. The flow rate of 1.0 cubic foot per minute (28 lpm) does not normally vary through the sampling period since constant pressure drop is maintained (no filtration occurs except for the backup filter, resulting in minimal pressure changes).

2.2 INSTRUMENT OPERATION AND ANALYSIS PROCEDURES

A collection medium of woven Teflon fiber "filter paper" is placed on the collection plate of each stage. The weights of the Teflon filters are determined prior to sampling under constant temperature and humidity conditions ($30^{o}C \pm 1^{o}$ and 50% relative humidity $\pm$ 1%) and before and after sampling are weighed on a microbalance. A plutonium radioactive source is used to eliminate static charge which may affect weighings. Extracts of the filters and of the tubes are analyzed for sulphate and nitrate content by ion chromatography and for ammonium ion colorimetrically.

Ion chromatography is a technique which employs ion exchange, eluent suppression, and conductometric detection to quantify levels of strong acid anions such as sulphate, nitrate, and chloride. In the ion chromatograph, a low-capacity separator column provides high efficiency separation on anions through competition of the anions and the eluent for active sites on the column. The degree of species separation and retention time depends on the relative affinities of different ions for the active sites, eluent strength and eluent flow rate. An eluent containing $NaHCO_3$ and Na_2CO_3 has been found to be particularly effective in the resolution of sulphate and nitrate ions, as well as other ions commonly found in aerosol filter samples and rainwater. After separation the eluent plus sample stream passes through a suppressor column which converts the eluent from a high conductivity form to a low conductivity form (H_2CO_3 in this case). The suppressor column is continuously regenerated. The anions of strong acids remain dissociated and are detected by means of their electrical conductivity. Detection limits are about 10 μg per liter or 0.005 $\mu g\ m^{-3}$ of air based upon a 24 h sampling period of 28 lpm with 20 ml of extracting solution per filter or tube.

The automated procedure for the measurement of ammonium ion employs the Berthelet reaction in which a blue colored compound (thought to be closely related to indophenol) is formed from the addition of an ammonium salt to a solution of sodium phenoxide, followed by addition of sodium hypochlorite. Sodium nitroprusside is added to enhance sensitivity. Also a potassium sodium tartrate solution is added to the sample stream to eliminate precipitation of hydroxides of any heavy metals which may exist in the sample solution. A Technicon Autoanalyzer II system is used to automate the analysis. The detection limit is about 0.02 mg l^{-1} of nitrogen or about 0.01 $\mu g\ m^{-3}$ of ammonium ion.

Filters from the dichotomous samplers can be weighed and analyzed for 33 elements by x-ray fluorescence spectrometry. The list of elements and the detection limit of each are given in Table 1. The detection limit defined by the standard deviation of the blank is 4.65. If the sampling period was 24 h, 40 m^3 of air would be sampled and the detection limit would be about 3 $\eta g\ m^{-3}$ for aluminium ion or 6 $\eta g\ m^{-3}$ for sulphur ion.

2.3 TESTING OF THE KAPS-IMPACTOR SYSTEM

Preliminary testing of the KAPS-impactor system was carried out during April 29-30, at the University of Calgary. The ambient outdoor atmosphere was sampled from 17:00 April 29 to 14:00 April 30, a period of 21 hours at a flow rate of 28 lpm. The KAPS sampling tubes were analyzed by ion chromatography for HNO_3, HNO_2, and SO_2, and colorimetrically for NH_3. Teflon filters were used to collect particles in the 2.1-3.3, 1.1-2.1, 0.7-1.1, and 0.4-0.7 μm size ranges and were analyzed for particulate NO_3^- and SO_4^{2-}. The results were as indicated in the following Table 2.

TABLE 1. X-Ray Fluorescence Analysis of Air Filters

List of Elements and Detection Limit

Element	Detection Limit (ηg per filter)	Element	Detection Limit (ηg per filter)
Al	130	As	20
Si	90	Se	20
P	70	Br	30
S	240	Rb	40
Cl	120	Sr	40
K	50	Y	50
Ca	40	Zr	120
Cr	10	Cd	170
Mn	20	In	210
Fe	30	Sn	210
Ni	20	Sb	210
Cu	20	Ba	1300
Zn	20	Lg	1300
Gg	20	Hg	40
		Pb	70

TABLE 2 Results of Field Test of KAPS-impactor System

Impactor Particulate Samples ($\mu g\ m^{-3}$ of air)

Filter Size Type	NO_3^-	SO_4^{2-}	
Blank Teflon Filter	0.0018	0.0104	
2.1-3.3 μm		0.0069	0.0369
1.1-2.1 μm		0.0092	0.0554
0.7-1.1 μm		0.0294	0.1837
0.4-0.7 μm		0.0454	0.1497

KAPS Gaseous Samples ($\mu g\ m^{-3}$ of air)

	HNO_2	HNO_3	SO_2	NH_3
KAPS Samples	0.383	0.235	1.01	2.8

The sampling period was generally cloudy with light snow flurries and pollutant concentrations in Calgary were below normal. Visual inspection of the filters indicated that most of the particles were in the 0.7 to 1.1 μm and the 0.4 to 0.7 μm size ranges. This was borne out by the chemical analysis which showed maximum concentration of sulphate in the 0.7 to 1.1 μm range and of nitrate in the 0.4 to 0.7 μm range. Thus the majority of the aerosol was in the accumulation size range, the range which affects visibility. Most of the pollutants measured were in a gaseous form. Nitrous acid concentrations were 0.383 $\mu g\ m^{-3}$ and nitric acid 0.235 $\mu g\ m^{-3}$ for a total of 0.75 $\mu g\ m^{-3}$ (reported as NO_3^-), as compared to 0.093 $\mu g\ m^{-3}$ NO_3^- in particulate form (NO_3^- may have existed in other not measured size ranges but this appears to be minimal.) Total SO_2 was 1.5 $\mu g\ m^{-3}$ (as SO_4^{2-}) as compared with 0.44 $\mu g\ m^{-3}$ detected on the filters.

2.4 CONCLUSIONS OF CHEMICAL SAMPLING TECHNIQUE DEVELOPMENT

The KAPS-impactor sampling system has been developed and tested. With it, particulate and gaseous pollutants can be separated and particulate aerosols can also be size fractionated. Results from the preliminary tests suggest that most of the nitrate and sulphate is found in fine particles, as expected.

3. ANALYSIS OF AIRCRAFT MEASUREMENTS OF AEROSOL PROFILES

A major component of Phase I was the comparative examination of the profiles of atmospheric aerosols upwind and downwind of the Calgary urban area as obtained from research aircraft data. The purpose of this examination was to demonstrate the potential of a suitably instrumented aircraft in obtaining air quality data. An additional goal was the devlopment of techniques and procedures for deriving estimates of the vertical distribution of aerosols and their visibility-reducing characteristics. As an example of the type of results obtainable from aircraft measurements, this section describes the results of case studies that examined the aerosol properties for an urban and a rural profile. These profiles were derived from selected existing aerosol data previously collected by the Intera/ARC research aircraft in central Alberta. These data were collected during the summers of 1983 and 1984 during research flights carried out on behalf of the Alberta Hail Project.

This section describes the results of this analysis of aerosol profiles. The research aircraft system is briefly noted followed by a discussion of the selection of the two case studies. Aerosol profiles for each of the cases are then examined and the vertical distribution of aerosol concentrations and size spectra compared. Mie scattering theory is then applied to the two aerosol profiles to derive estimates of the vertical distribution of the aerosol light extinction coefficient.

3.1 AIRCRAFT INSTRUMENTATION AND AEROSOL SAMPLING PROCEDURES

The Alberta Research Council research aircraft facility has been developed in conjunction with Intera Technologies Ltd. This facility is based on a Cessna Conquest twin-engine turboprop aircraft with a data acquisition system capable of measuring and recording a variety of atmospheric parameters (Cheng et al., 1986). Presently, data collected comprise state parameters including temperature, pressure and humidity, images of ice crystals and precipitation

particles, extensive wind and turbulence information, and size and concentrations of aerosols.

The Intera/ARC research aircraft measures aerosols using an Active Scattering Aerosol Spectrometer Probe (ASASP) manufactured by Particle Measuring Systems Inc. This probe, which is mounted on a rack under the belly of the aircraft, is designed with a single size range divided into fifteen linear size intervals. The ASASP is capable of sizing particles within the useful range of 0.12 to 3.12 μm diameter with size intervals of 0.025 μm. The instrument operates on the principle that the light scattered by a particle within an active laser cavity is directly proportional to its size. While the laser optical probe provides the size and concentration of particles, it will not give the chemical properties of the aerosols.

Most of the existing data collected by the research aircraft are in the Red Deer region and explicit profiles for the Calgary region were not readily available. Examination of the existing data sets indicated occasional refuelling stopovers were made at the Calgary International Airport during the summers of 1983 and 1984. These profiles were therefore selected as the downwind profile representing the urban case. As no flights were completed upwind of Calgary, landings and takeoffs at the Red Deer Industrial Airport were selected as providing aerosol data for the rural setting. These latter cases were considered analogous to the upwind conditions at Calgary.

Examination of the existing flight cases revealed that there were few cases with data in the Calgary region that were suitable for analysis. On many flights conducted during the two summers aerosol data were not recorded. Of the Calgary stopovers, only the landing of 22 June 1983 provided a complete vertical profile of urban atmospheric aerosols. No aerosol measurements were recorded on landings or takeoffs at the Red Deer airport for this day, therefore same day comparisons can not be made between urban and rural vertical profiles in this study using past years data. Thus data from 13 July 1984 will be presented as the rural case.

3.2 URBAN AEROSOL PROFILE CASE STUDY (JUNE 22, 1983)

The flight of 22 June 1983 approached Calgary at an altitude lower than 2100 metres mean sea level (msl). This limited the measurement of the urban aerosol profile to that below the 770 millibar (mb) pressure level height. Aerosol profile measurements started within a few metres above ground level and extended to the 770 mb pressure level. All aerosol measurements were made in clear air conditions.

The aerosol particle concentration profile for the urban setting is shown in Figure 2, with the corresponding soundings of relative humidity and equivalent potential temperature shown in Figure 3. These profiles were recorded at 14:00 local daylight saving time (MDT). Figure 2 shows the particle concentration from ground level up to 200 metres was between 500 and 600 cm^{-3}. The concentration increased greatly with increasing elevation above ground, reaching a maximum of about 850 cm^{-3} at approximately the 850 mb level (1350 metres msl). A continuous decrease in concentration with increasing altitude followed. The profiles of relative humidity and equivalent potential temperature also display a sudden change at the 1350 metres msl altitude. This discontinuity represents the top of the mixing layer.

3.3 RURAL AEROSOL PROFILE CASE STUDY (JULY 13, 1984)

Shown in Figure 4 is the rural aerosol particle concentration profile taken on 13 July 1984 at 17:00 MDT. The soundings of relative humidity and equivalent potential temperature corresponding to this profile are shown in Figure 5. The concentration in the lowest 200 metres of the profile is less than 400 cm^{-3} and then increases very gradually with increasing height. Relative humidity also increases gradually with height, while the equivalent potential temperature indicates neutral stability.

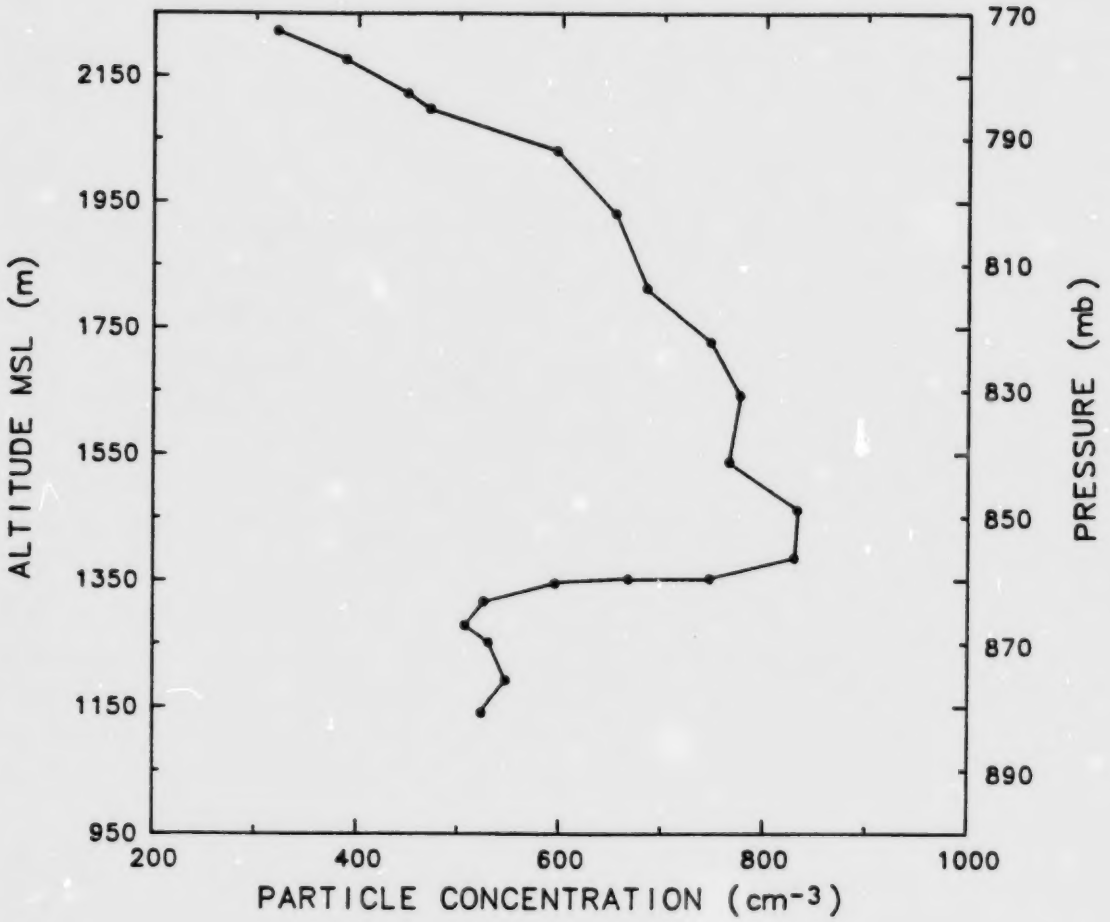

Figure 2. Aerosol Particle Concentration Profile for Calgary, 22 June 1983.

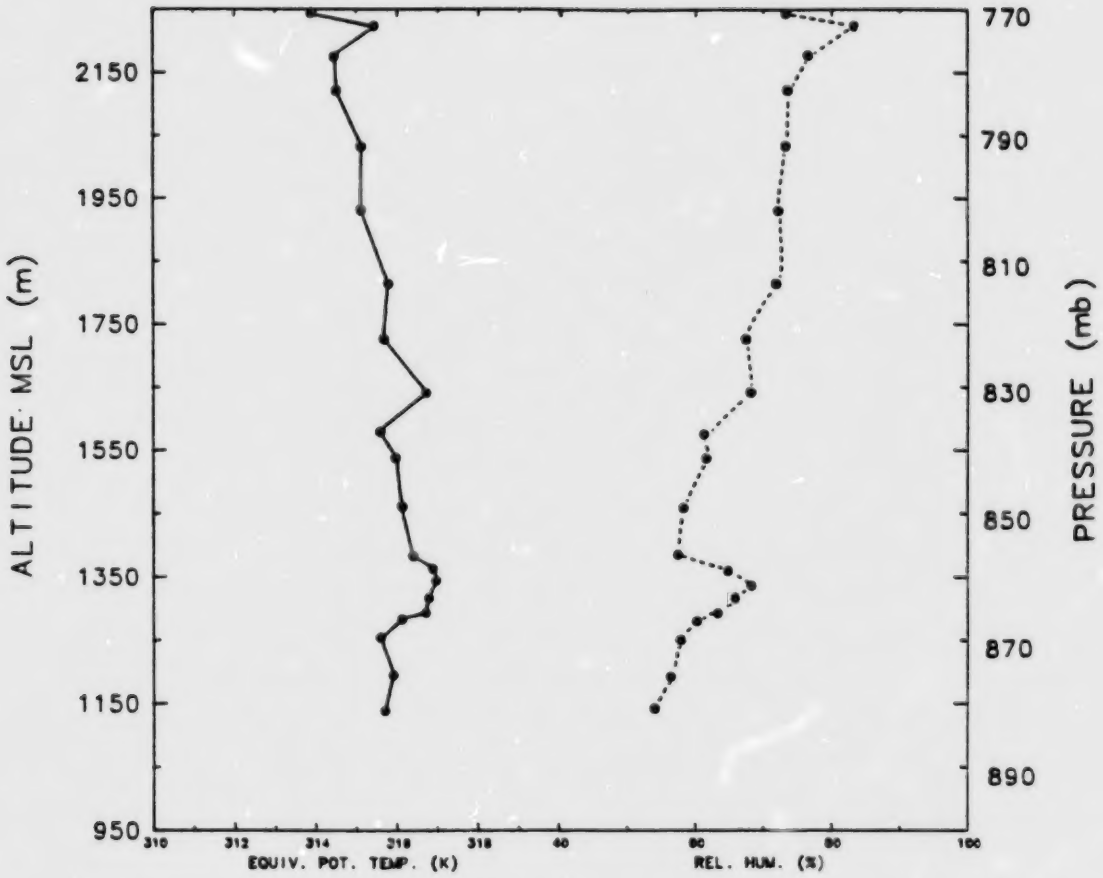

Figure 3. The Relative Humidity and Equivalent Potential Temperature Profiles for Calgary, 22 June 1983.

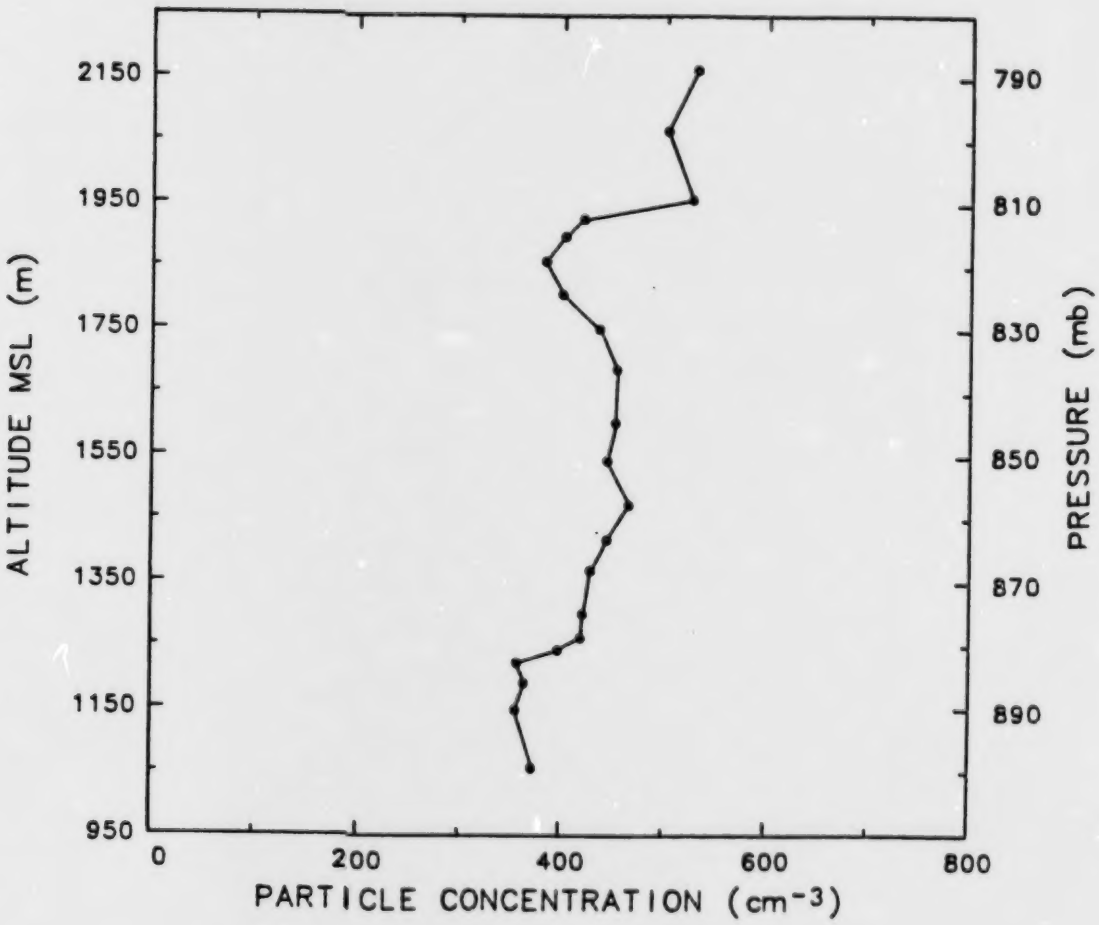

Figure 4. Aerosol Particle Concentration Profile for Red Deer Industrial Airport, 13 July 1984.

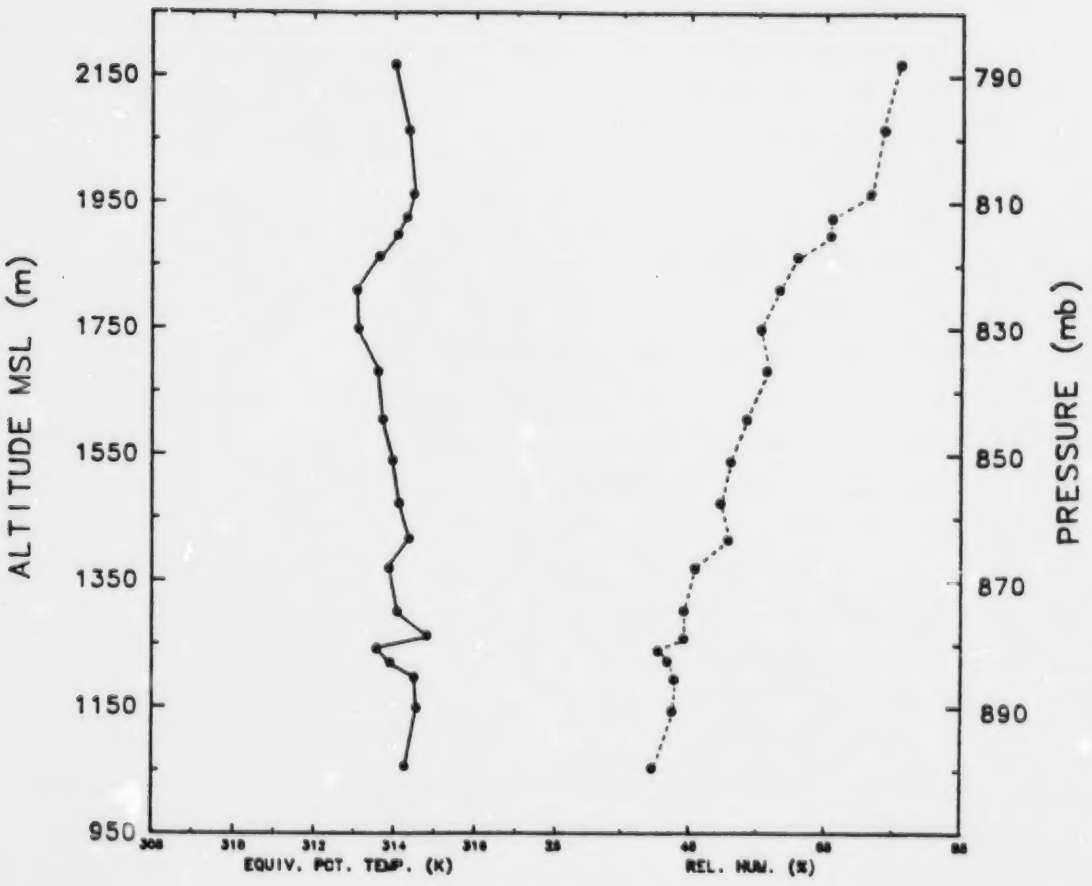

Figure 5. The Relative Humidity and Equivalent Potential Temperature Profiles for Red Deer Industrial Airport, 13 July 1984.

The aircraft, on 13 July 1984, passed through cloud at 3100 metres msl on approach to the Red Deer airport from an altitude in excess of 3 km above ground. Maximum aerosol particle concentrations, of greater than 600 cm^{-3}, were found to be located just below cloud base and then decreased to about 50 cm^{-3} at a height of 3500 metres msl. Isaac, et al., (1985) reported similar vertical aerosol particle profiles where concentrations reached their maximum below cloud base. This was thought to be linked directly to cloud presence and not due to hygroscopic growth.

3.4 COMPARISON OF URBAN AND RURAL PROFILES

The aerosol number concentration, extinction efficiency for various aerosol radii, and extinction coefficient due to scattering and absorption by aerosol were determined, using 5 second ASASP averages, at 10 mb intervals from ground level to 770 mb. The sampling period of 5 seconds was used because the aircraft was always ascending or descending and the altitude of measurement needed to be clearly defined. Shown in Figures 6 and 7 are the number concentration spectra for the urban and rural situations at three levels, ground level, 850 mb and 770 mb. Where concentrations became too low for any accurate measurement over the averaged sampling period, the spectra were terminated. The spectrum with the largest values for Calgary is the one corresponding to the 850 mb level, followed by the ground level and 770 mb level spectra. This coincides with the aerosol particle concentration profile in Figure 2 where the highest concentrations occur around the 850 mb pressure level. For the rural situation the spectrum with the largest values is the one corresponding to the 770 mb level, which was close to cloud base, followed by the 850 mb and ground level spectra.

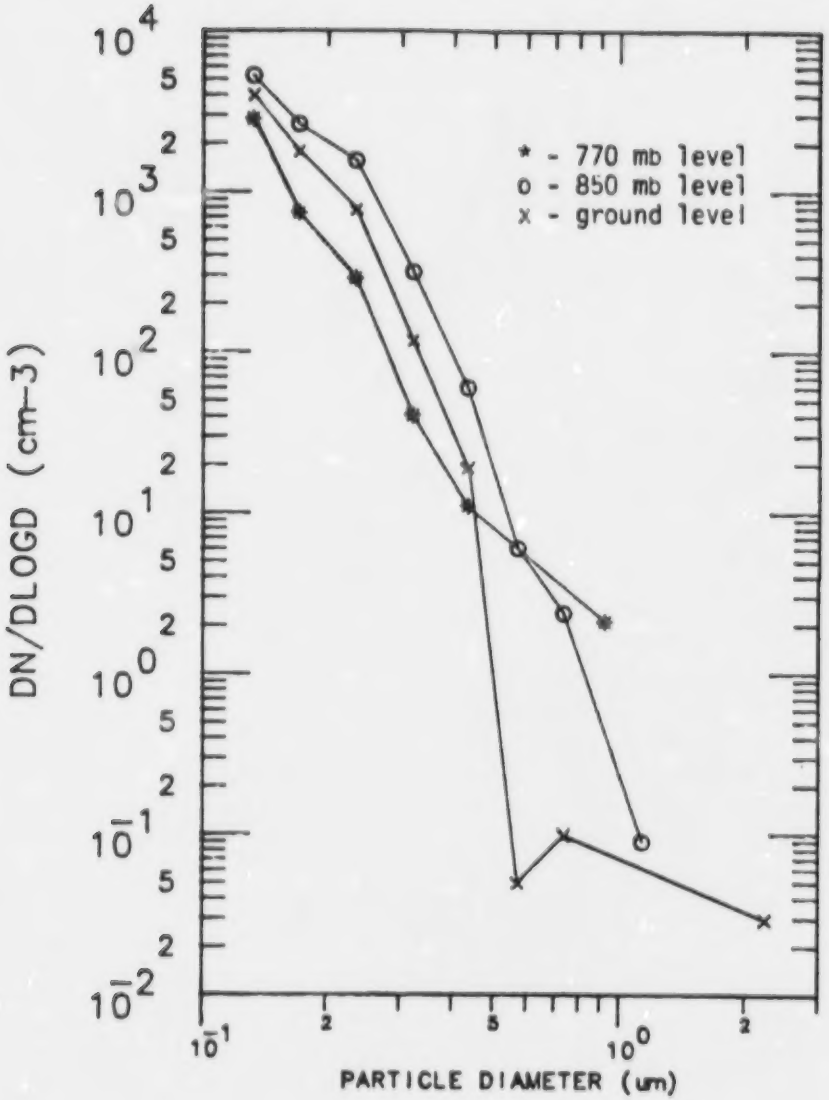

Figure 6. Aerosol Particle Concentration Spectra for Three Levels, 770 mb, 850 mb and Ground Level for Calgary, 22 June 1983.

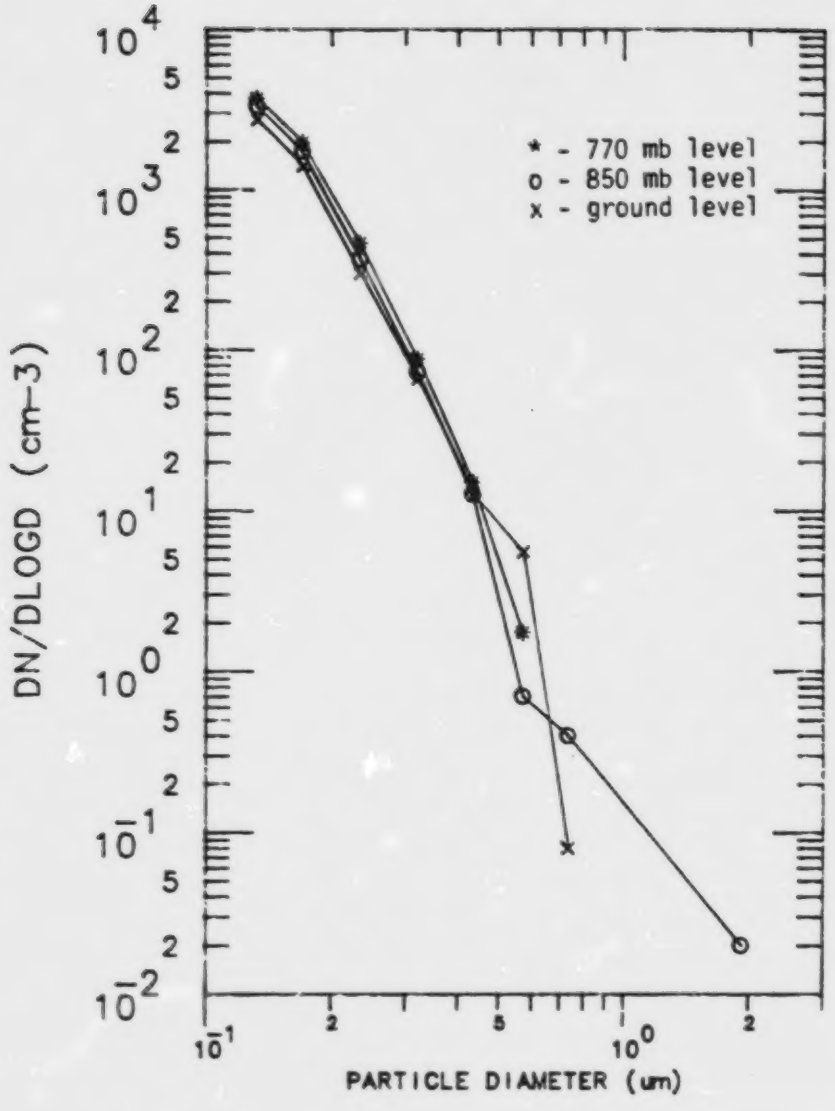

Figure 7. Aerosol Particle Concentration Spectra for Three Levels, 770 mb, 850 mb and Ground Level for Red Deer Industrial Airport, 13 July 1984.

3.5 CALCULATED VERTICAL DISTRIBUTION OF AEROSOL EXTINCTION

The total amount of light which is scattered or absorbed depends upon the particle radius, the wavelength of visible light and the index of refraction of the particle. Chemical composition of the particle determines the index of refraction. In this study, particles are assumed to be composed of either ammonium sulphate ($(NH_4)2SO_4$), ammonium bisulphate (NH_4HSO_4) or sulphuric acid (H_2SO_4), with indices of refraction of 1.523, 1.473 and 1.437 μm respectively. The wavelength used for all computations was 0.55 μm, which is approximately in the middle of the visible light band.

Mie theory is used to determine the scattering and absorption of light by spherical particles and its numerical application has been extensively discussed by Kerker (1969). A computer program to compute Mie scattering coefficients for coated spheres, developed by Bohren (1983), was used for the analysis of the aerosol data collected by the research aircraft. Bohren's program, called BHCOAT, can be used for a homogeneous sphere, as is assumed in this analysis, if the values for the refractive indices for both inner and outer sphere are given to be equal.

The extinction efficiency (Q_{ext}) due to scattering and absorption by a particle is strongly dependent on the size parameter $\hat{\alpha}$, which is defined as $\hat{\alpha} = 2\pi r/\lambda$ where r is the particle radius and λ is the wavelength of light. Figure 8 shows the extinction efficiencies versus size parameter for the three aerosol types assumed. For smaller particles there is a sharp rise in the extinction efficiency as the particle size increases. As the particle size continues to increase the efficiency decreases. This oscillation continues, but its intensity is reduced as the size parameter increases. The total extinction coefficient (b_{ext}) can be expressed as:

$$b_{ext} = \int n(r)\, Q_{ext}\, \pi r^2\, dr \qquad (4.1)$$

where n(r) is the particle size distribution.

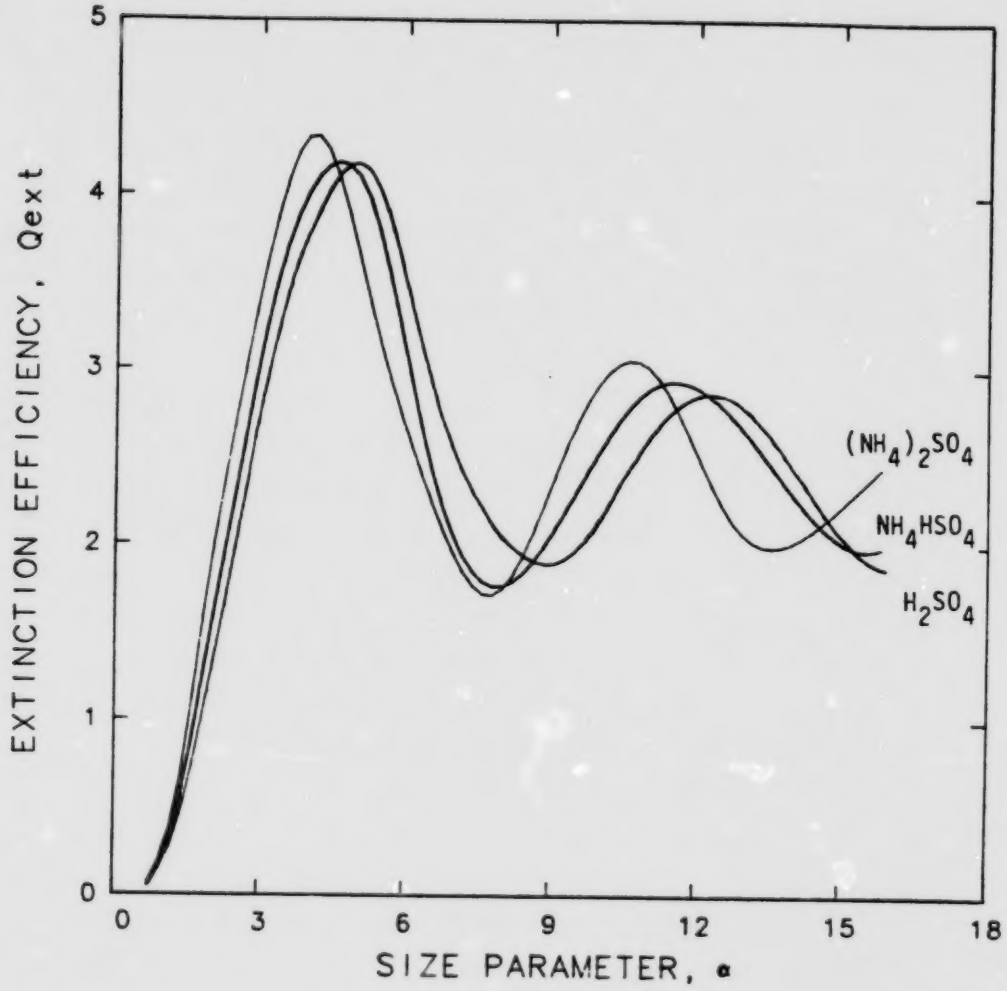

Figure 8. Extinction Efficiency versus Size Parameter for Ammonium Sulphate, Ammonium Bisulphate and Sulphuric Acid Spheres using a visible light wavelength of 0.55 um.

Vertical profiles of the total extinction coefficient were derived using Equation 4.1 and the measured aerosol size concentrations. Figures 9 and 10 show the shaded "envelope" of calculated extinction values for the urban and rural aerosol data respectively. The left side of the shaded region represents the results for dry ammonium sulphate and the right side the results for dry sulphuric acid. The calculated extinction values for ammonium bisulphate lie between these two limits. The results show that the rural extinction coefficient values are lower than the urban values for all levels, except for altitudes above 790 mb.

3.6 CONCLUSIONS AND DISCUSSION OF AIRCRAFT DATA ANALYSIS

Existing aerosol data collected by the Intera/ARC research aircraft has been examined and examples of rural and urban vertical profiles of aerosol concentration have been derived. These sample profiles show that the vertical distribution of aerosols can differ quite dramatically with location and meteorological conditions. The sample profiles have also been used to calculate the extinction efficiencies using a numerical model of Mie scattering and assumed aerosol chemical characteristics.

Although aerosol vertical profiles are of prime importance in a study of the effect of urban air quality on visibility, other data obtainable with a suitably instrumented aircraft could also be useful. For example, the aircraft can be equipped with gas analyzers, filter packs and radiometers. Most of this instrumentation has been employed on the Intera/ARC research aircraft on previous studies (Cheng et al., 1986). Aside from the Intera/ARC aircraft, a number of other aircraft with the appropriate instrument configuration are also currently operating in Canada and the United States.

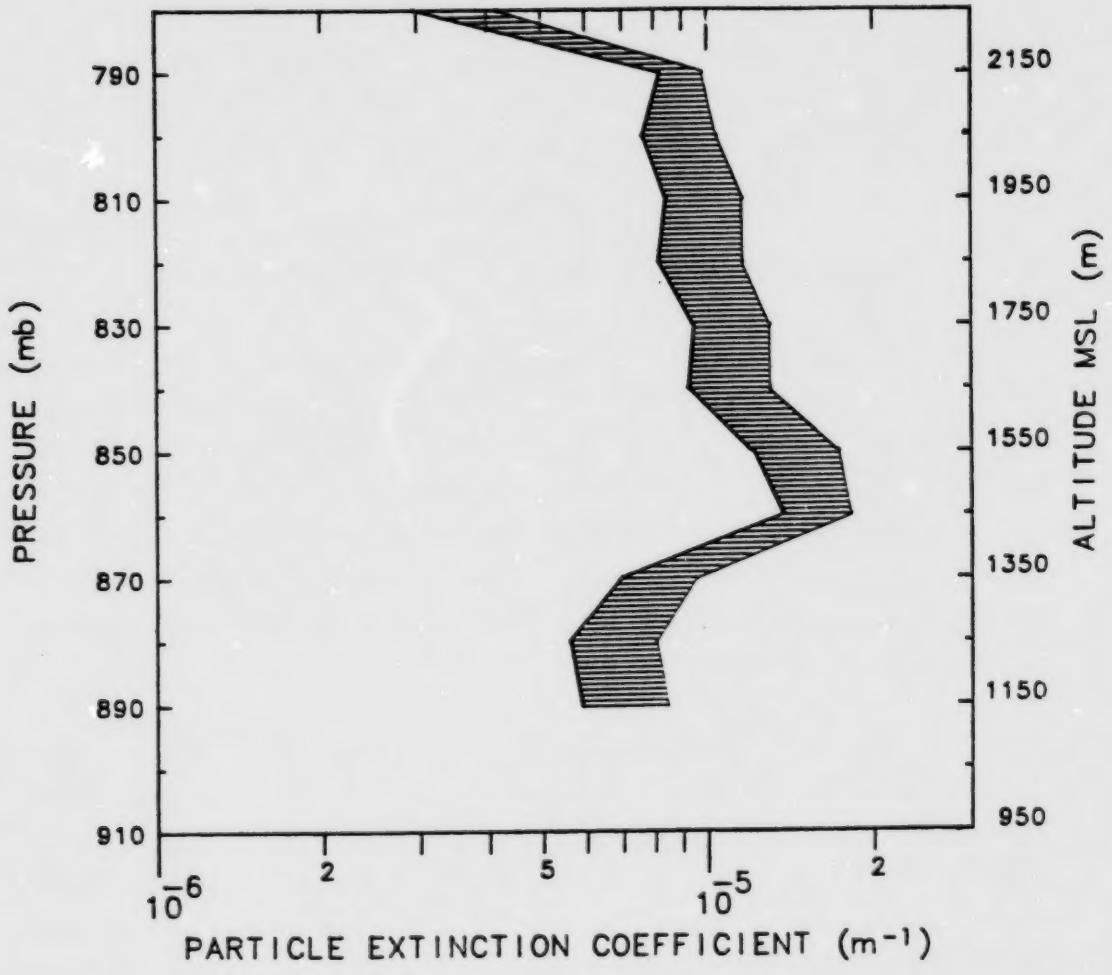

Figure 9. Particle Extinction Coefficient Profiles (visible wavelength 0.55 um) for Calgary, 22 June 1983.

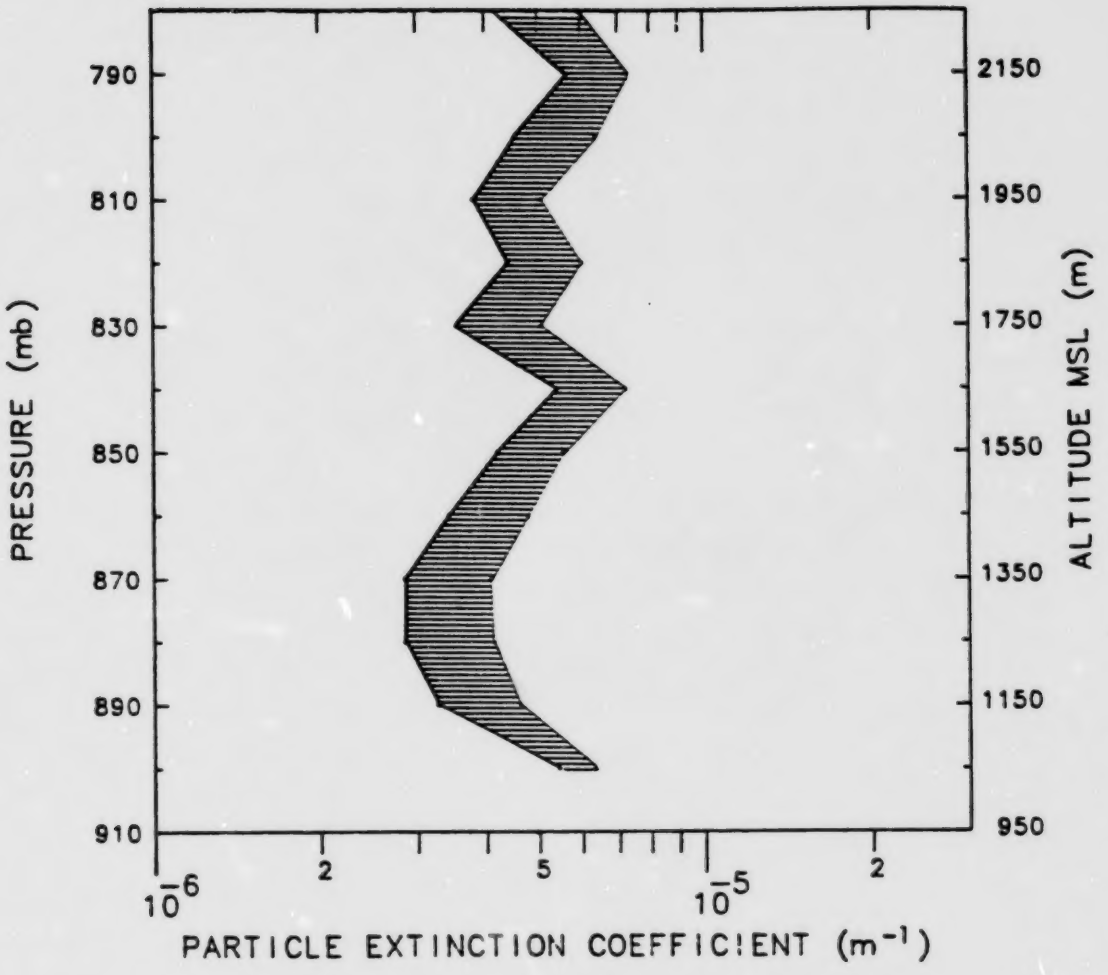

Figure 10. Particle Extinction Coefficient Profiles (visible wavelength 0.55 um) for Red Deer Industrial Airport, 13 July, 1984.

4. IRRADIANCE MEASUREMENT PROGRAM AND AEROSOL TURBIDITY

The objective of the Phase I radiation measurement program was to develop instrumentation and procedures for monitoring the Calgary atmospheric aerosol load. These techniques would use radiometric measurements and radiation modelling to determine the aerosol characteristics that affect the visibility and radiation balances of the Calgary urban environment. This approach would have as its goal the calculation of the vertically integrated "aerosol optical depth" as the expression of this aerosol loading.

This section briefly states the theoretical basis of the radiometric approach for determining atmospheric aerosol loadings. This is followed by a presentation of the basics of the solar irradiance model applied for optical depth determination. The radiation instrumentation installed in Calgary and the field measurement program are then described. Results of the program are then presented along with an analysis of selected data. The section closes with a summary of the results and conclusions about the program and procedures used.

4.1 AEROSOL OPTICAL DEPTH

Atmospheric turbidity can be expressed by the aerosol optical depth $\tau_a(\lambda)$ and by the aerosol volume extinction coefficient $b_{ext}(\lambda,z)$ which are related as follows:

$$\tau_a(\lambda) = \int b_{ext}(\lambda,z)\, dz \qquad (5.1)$$

A spectrally averaged approximation for mean aerosol optical depth can be expressed as:

$$\tau_a = \int b_{ext}(z)\, dz \qquad (5.2)$$

Thus $b_{ext}(z)$ indicates extinction due to aerosol at a certain height z, whereas τ_a integrates the effects of extinction over the entire vertical column of the atmosphere.

Explicit determination of τ_a requires a knowledge of $b_{ext}(z)$ at all heights z, which would require aircraft observations. An alternative approach is the residual calculation of the aerosol optical depth using solar irradiance measurements and modelled values of irradiance for an aerosol-free atmosphere (Unsworth and Monteith, 1972). This technique has been applied for a variety of urban and non-urban sites within Canada (Barlow, 1979; Freund, 1983; Uboegbulam and Davies, 1983; Davies and Stewart, 1984).

Calculation of the aerosol optical depth can be made by means of the equation of transfer for direct solar irradiance (Paltridge and Platt, 1976):

$$I = I_o \cos\Theta\, (T_{oz} T_R - a_w) \exp(-\tau_a m_r) \qquad (5.3)$$

where: I is direct solar irradiance on a horizontal surface, I_o is the solar irradiance at the top of the atmosphere, Θ is the solar zenith angle, T_{oz} is the transmissivity of atmospheric ozone, T_R is the transmissivity of molecular (Rayleigh) scattering, a_w is water vapour absorption, and m_r is the relative optical air mass.

Rearrangement and simplification of (5.3) yields an expression for aerosol optical depth:

$$\tau_a = (-1/m_r) \ln (I_m/I_c) \qquad (5.4)$$

where I_m is the measured direct beam solar irradiance at the surface and I_c is the calculated surface irradiance for an aerosol-free atmosphere. I_c values can be calculated using appropriate models and parameterized expressions for the transmission and absorption terms of (5.3) (Davies and Hay, 1980).

Thus a measurement of atmospheric turbidity of Calgary, as expressed by τ_a, can be derived from radiation measurements and modelled values. This turbidity measure is related to the visibility expression (Equation 1.2) and comparisons to reported visibility range can be made. The relationship between aerosol particle mass loading, atmospheric attenuation and visibility degradation would be derived from these measurements.

4.2 RADIATION MODEL

The direct beam irradiance model values for an aerosol-free atmosphere were calculated using Equation 5.3 expressed without the aerosol transmission term:

$$I_c = I_o \cos\Theta (T_{oz} T_R - a_w) \qquad (5.5)$$

The application of the model requires expressions for extra-terrestrial irradiance, I_o, and the transmission and absorption terms; T_{oz}, T_R, and a_w. These can be expressed by parameterizations based on measured or assumed atmospheric constituents and solar position.

For model use, expressions for the various terms were selected from parameterizations noted in the literature and used in similar direct-beam models (Barlow, 1979; Davis and Hay, 1980; Freund, 1983). Solar position can be accurately described by mathematical approximations of the earth-solar radius vector and time (McCullogh, 1968). A recently derived value of the solar constant of 1376 Wm^{-2} has been used (Hickey et al., 1980) for an assumed extraterrestrial irradiance value, I_o. Transmissions are functions of a generalized attenuator pathlength, defined as the product of vertical column amount and the relative air mass, m_r. Attenuator amount must be calculated or specified while the model value of m_r is accurately expressed by the pressure-corrected Kasten (1966) formula.

Ozone transmission, T_{oz}, was calculated using the Lacis and Hansen (1974) parameterization of absorption for a specified value of an ozone pathlength. Ozone pathlength is derived from the specified vertical amount of ozone scaled by an appropriate air mass term (e.g., Rodgers,1967). The Lacis and Hansen approximation is suggested to be accurate to within 0.5 %. It can be assumed that the accuracy of the transmission parameterization exceeds the accuracy of ozone measurement or specification.

An estimated value of atmospheric ozone for all model calculations was made from tabled values of climatological averages (Dutsch, 1969). The average climatological monthly values for March and April for the Calgary latitude (51^{o} N) was estimated to be 0.400 atmo-cm. The model is relatively insensitive to ozone values and this assumption is not considered to greatly affect calculated values.

Absorption by water, carbon and diatomic oxygen was calculated using the Lacis and Hansen (1974) approximation of the Yamamoto (1962) curves. This approximation requires specification of atmospheric precipitable water. The estimated accuracy of this approximation is 1% for most situations.

Molecular (Rayleigh) scattering is a function of the pressure-corrected air mass, m_r, and was determined using interpolations of previously derived curves (Barlow, 1979). These curves were derived from the use of Elterman's (1968) molecular number density data and the solar spectral values of Thekaekara (1973). These values were calculated for a U.S. Standard Atmosphere 50 km in depth and divided into 1 km layers. A cubic spline interpolation procedure was used for routine model calculations, with an expected error of less than 0.01% compared to tabled values.

4.3 MODEL OF SPECTRAL AEROSOL OPTICAL DEPTHS

Spectral optical depths for aerosols were also examined as a means of determining urban aerosol characteristics. These values can be determined using spectral irradiance measurements derived from special Schott filters combined with appropriate spectral model estimates. Model values of the spectral optical depths were calculated using the following expression:

$$\tau_a(\lambda) = (1/-m_r) * (I_m(\lambda)/I_c(\lambda)) \qquad (5.6)$$

where $\tau_a(\lambda)$ is the aerosol optical depth for the defined spectral band and $I_m(\lambda)$ and $I_c(\lambda)$ are the measured and calculated average irradiance values for the spectral bands.

Modelled irradiance values were derived using the following expression:

$$I_c(\lambda) = I_o(\lambda) * T_R(\lambda) * T_{oz}(\lambda) \qquad (5.7)$$

where $I_o(\lambda)$, $T_R(\lambda)$ and $T_{oz}(\lambda)$ are extra-terrestrial irradiance, Rayleigh transmission, and ozone transmission values for the spectral band. The equation explicitly does not include molecular absorption as this is not a major factor for the selected spectral bands.

Irradiance and molecular transmission values were derived from the Thekaekara (1973) and Elterman (1968) estimates respectively. Mean values for the band were determined by calculating the appropriate values at the lower and upper cutoffs of the narrow spectral band and then taking the arithmetic average as the representative values. These estimates were made using computer cubic spline fits to the cited standard data sets and then calculating the values at the appropriate boundary wavelengths.

Ozone optical depths were calculated using the Lacis and Hansen (1974) approximation for the weak absorption bands in the visible wavelengths. As with the broad band model, a climatological estimate of ozone (0.400 atmo-cm) was used in conjunction with an appropriate expression for ozone pathlength (Rodgers, 1967) for modelling purposes. While the above expression is a broad band estimate, the minor importance of ozone absorption at the spectral bands used would indicate sufficient accuracy for modelling use.

4.4 RADIATION MEASUREMENT PROGRAM

A radiation measurement system was installed on the roof of the Alberta Research Council office in Calgary, located off the Deerfoot Trail west of the airport, during February 17 - 19, 1986. The following instruments were installed:

1. One Kipp and Zonen pyranometer for measurement of global solar irradiance.

2. One Kipp and Zonen pyranometer and A.E.S.-type design occulting ring (diffusograph system) for measurement of diffuse solar irradiance.

3. One Eppley Normal Incidence Pyrheliometer and equatorial sun-tracker for measurement of direct-beam solar irradiance.

4. One Middleton net radiometer and air purging system for measurement of net (solar and thermal) irradiance.

In addition, an anemometer was installed on February 28, 1986 to assist in the assessment of irradiance measurement conditions. All data were logged using a Campbell Scientific 21x micrologger and stored on cassette tape. This instrument site was close to Calgary International Airport (YYC) and permitted use of the standard meteorological measurements made by A.E.S. On-site monitoring was provided by Alberta Research Council personnel.

Measurements were made continuously from mid-February until April 8. In addition, a special spectral measurement program was completed between April 8 and 9 during which the pyrheliometer was used for filter measurements. Instruments generally operated without failure throughout the period. However, a data storage overrun caused data not to be logged for the period approximately from noon on March 29 to noon on March 31. For the testing purposes reported here, those measurements made after March 1st inclusive were selected. This selection was due to a change on February 28 in the data micrologger program that simplified the archiving procedure but altered the data format. The systems were operated without mechanical failure for the entire period and all data are available as required.

Global, direct beam, diffuse and net irradiance values were sampled continuously at ten-second intervals and one minute averages, hourly averages and hourly integrated values were logged. In addition, 10 minute samples of wind direction and velocity were recorded.

The measurement accuracy of these instruments varies according to instrument type. A conservative estimate of total system accuracy of 5% is suggested for the two Kipp and Zonen radiometers and the net radiometer. This is consistent with reported assessments of the instrumental accuracy (Latimer, 1972). Manufacturer's specifications for the pyrheliometer indicate the instrument to be within 0.5% of the International Pyrheliometric Scale. For this study, a conservative estimate of 2% was adopted. All instruments were calibrated at the National Radiation Centre of the Atmsopheric Enviroment Service during June and July of 1985.

The hourly integrated values of irradiance during assumed cloud-free periods were selected from the continuous measurement data for calculation of hourly aerosol optical depths. Cloud-free hours were identified from the hourly meteorological observations made at the Calgary International Airport A.E.S. weather office.

A computer procedure for the automatic logging of A.E.S. hourly surface and pibal data for the Calgary International Airport station and upper air data for Edmonton was implemented on the ASD VAX 11/750 computer in Red Deer for the duration of the program. These data were used for irradiance modelling and visibility comparisons. Meteorological data since February 22 have been abstracted from the hourly observations at the A.E.S. station at Calgary International Airport. In addition, a computer procedure for the identification of clear sky conditions was developed.

A numerical procedure for the calculation of atmospheric precipitable water was developed for the project. This procedure used the radiosonde sounding from the A.E.S. upper-air station from Edmonton for calculating the total amount of atmospheric precipitable water. This quantity was used for determination of the molecular absorption term of Equation 5.5 in the calculation of irradiance. Values were determined for both the 0000Z and 1200Z soundings. For model application, the mean value for the two soundings bracketing the

time of model calculations was used as the representative value. Both the cloud identification program and the precipitable water procedure were applied to all meteorological data. Computer graphical procedures were developed for the display of irradiance data.

4.5 SPECTRAL MEASUREMENT PROGRAM

Selected spectral measurements of direct beam irradiance were made at the conclusion of the field measurement program. The purpose of these measurements was to test the use of spectral measurements for the derivation of narrow spectral band measurements of aerosol optical depth.

Measurements of direct solar fluxes were made with the Eppley pyrheliometer. This instrument has the capability of making spectral measurements by using a filter wheel at the end of the instrument tube fitted with Schott glass filters. This configuration permits the measurement of irradiance above the cutoff wavelength of each filter by rotating the wheel for multispectral viewing.

A limited field measurement program was conducted on April 8 and 9. A total of eight spectral filters were used to define six different spectral bands. For analysis purposes, the four middle bands were selected as having the most confident measurement accuracy. Table 3 indicates the bands derived by the combination of their filter expressions. By subtraction of the upper from the lower filter readings (after application of the appropriate filter factors), the values for the specified band fluxes were determined. These were interpreted as the monochromatic equivalent flux at an appropriately weighted central wavelength, $\hat{\lambda}$.

TABLE 3. Spectral Bands (μm) Determined By Schott Filters

FILTER EXPRESSION	LOWER λ	UPPER λ	$\Delta\lambda$	$\hat{\lambda}$
GG22 - GG14	.402	.492	.090	.450
GG14 - OG1	.492	.530	.038	.510
OG1 - RG2	.530	.623	.093	.576
RG2 - RG8	.623	.688	.065	.655

4.6 RESULTS OF RADIATION MEASUREMENT PROGRAM

4.6.1 Field Measurements of Irradiance Components

The results of the measurement program are given in Figures A.1 through A.8 in the appendix. Each of these figures shows a time series of hourly totals of irradiance (kJ/m^2) for a five-day sequence starting from March 1 through the end of the program on April 8. Included on the graphs are plots of the measured global, direct and diffuse irradiance values.

The characteristics of these hourly time-series plots are discussed in the appendix. This section will limit itself to the analysis of more detailed examples of the daily radiation regime under different cloud conditions. Representative examples are given in Figures 11 and 12 for days characterised by broken (March 8) and

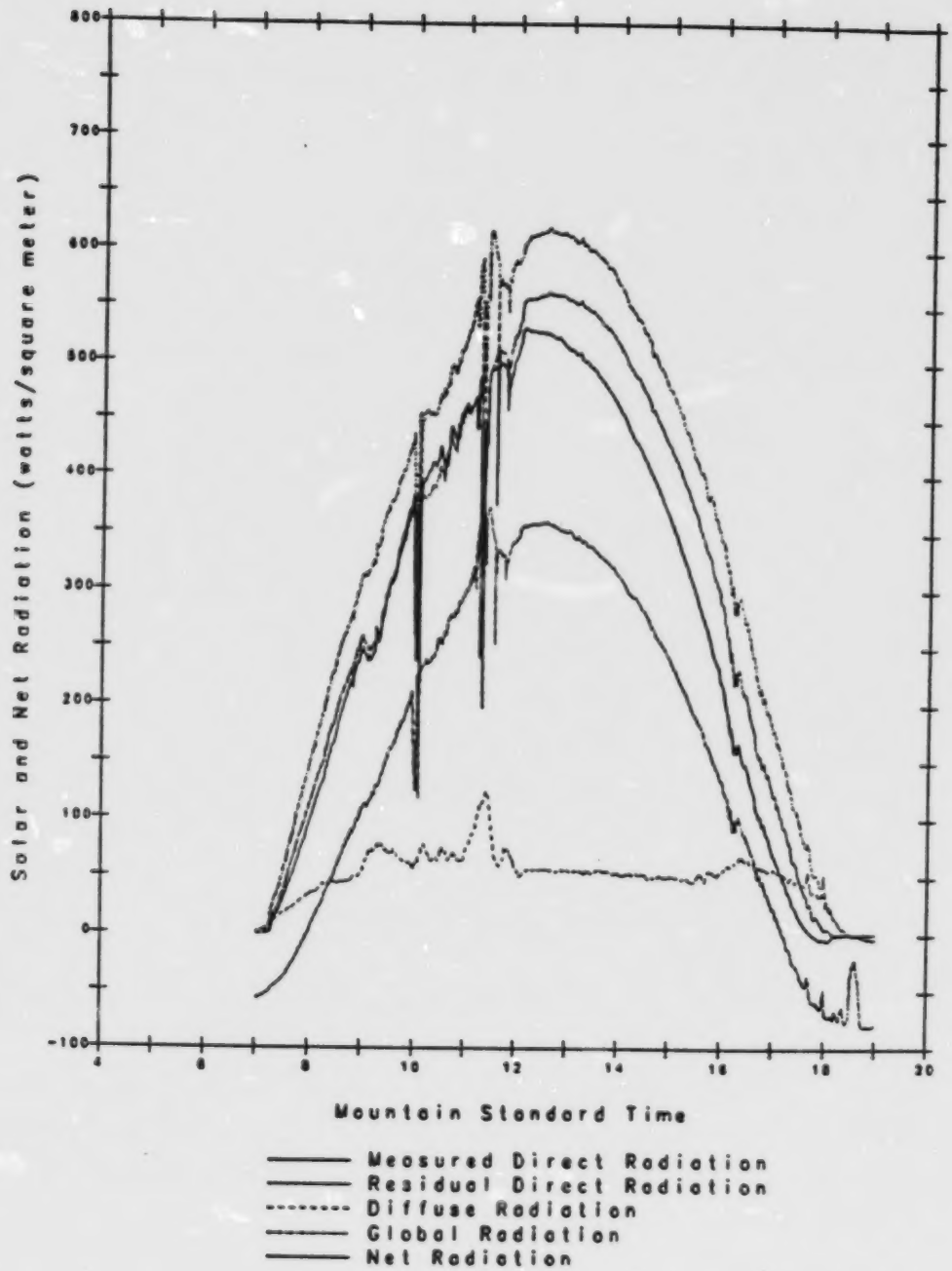

Figure 11. Solar and Net Radiation for March 8, 1986 (one-minute averages). Broken Cloud Conditions.

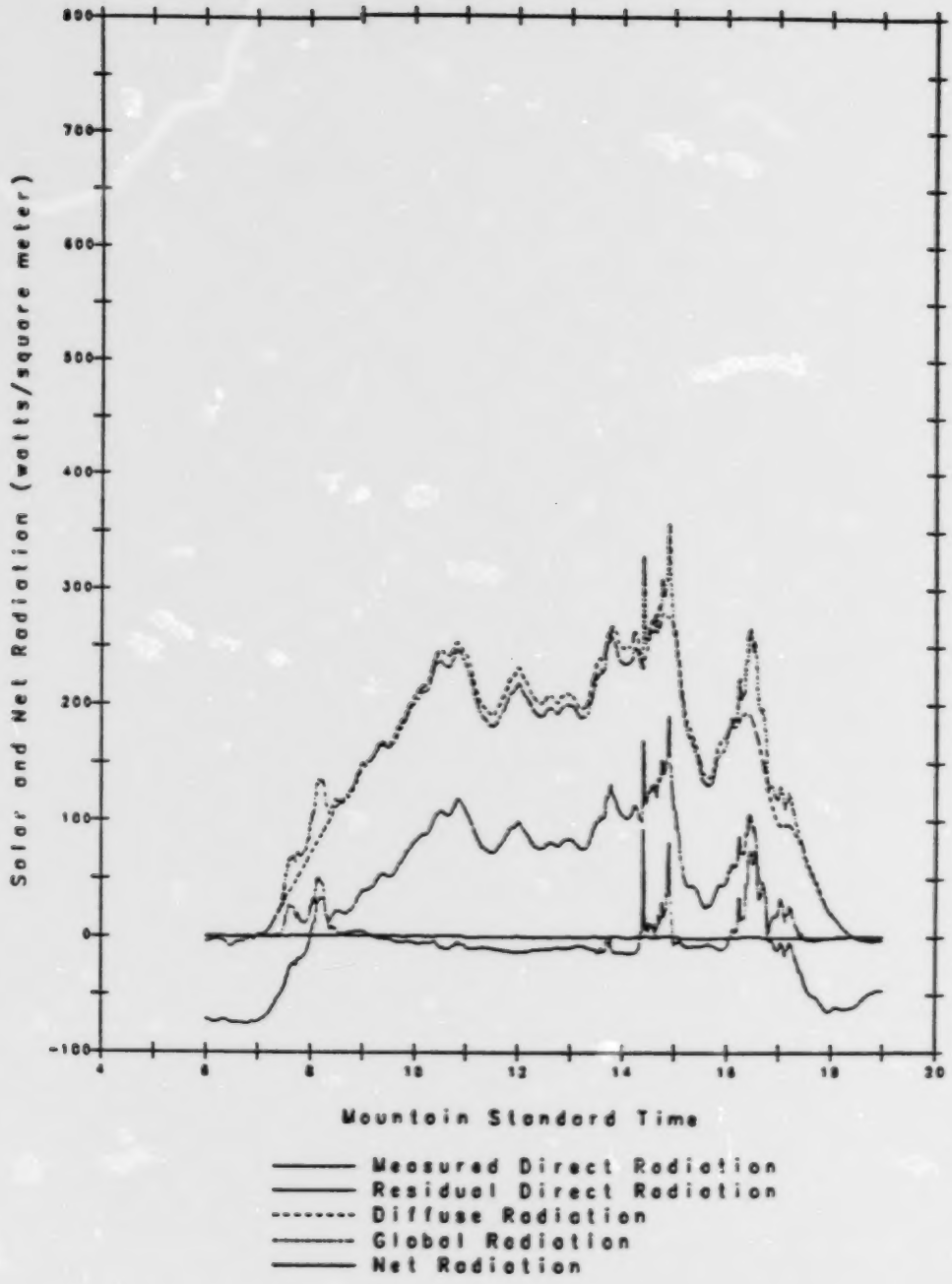

Figure 12. Solar and Net Radiation for March 9, 1986 (one-minute averages). Overcast Cloud Conditions.

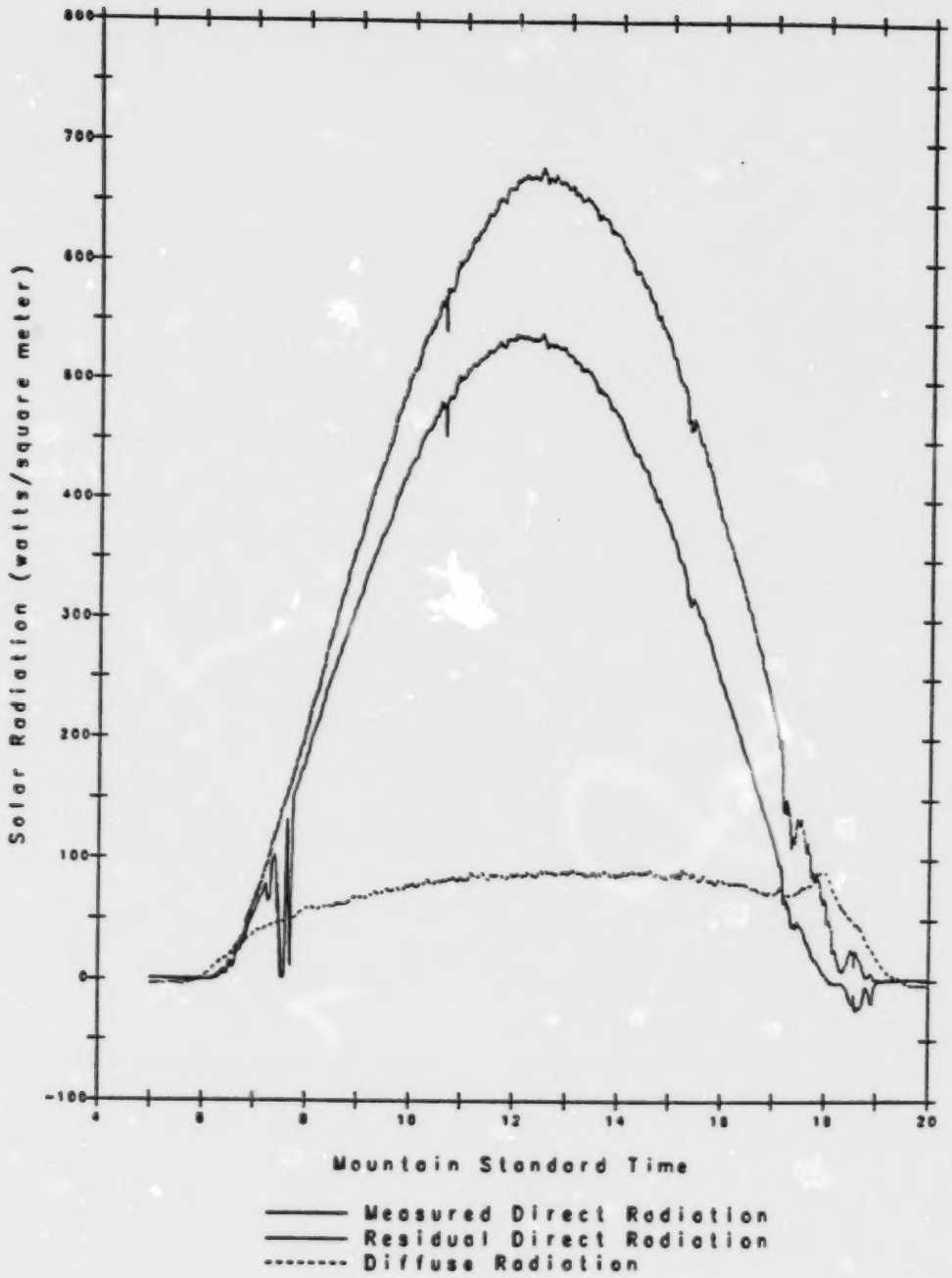

Figure 13. Solar Radiation Direct and Diffuse Components for April 7, 1986 (one-minute averages).

overcast (March 9) cloud conditions. These figures show the daily time series of one-minute averaged values (watts/m^2) for the global, direct, diffuse and net irradiance components. The effect of cloud cover is very apparent in the overcast case where measured direct beam irradiance is effectively zero and the global value is entirely diffuse. During the broken-cloud day, the transition from cloud to cloud-free optical path around noon is apparent. Earlier in the morning, the curves show depletion by cloud of the direct component and a coincident increase in diffuse values. A slight additional cloud-induced attenuation is apparent late in the afternoon.

In both cases, net radiation tracks the dominant solar component throughout the daylight hours. At night the net values become negative indicating the loss of thermal radiation expected at night. The insulating role of nocturnal cloud cover is suggested in the slightly reduced radiative losses indicated after sunset.

A final example is shown in Figure 13 for the "clear-sky" case of April 7, 1986 when no significant cloud cover was present. This example is limited to the direct and diffuse solar components. The curve shows an abrupt early morning discontinuity in the pyrheliometer-measured direct values between 0700 and 0800 hours. This is due to a blockage of the instrument sensing aperture by the wrapped signal cable. After correction at 0800 hours, the pyrheliometer values continue to track the residually-derived direct values. Differences in both types of direct beam measurement become larger after 1000 hrs and become asymmetrical in the afternoon hours. This difference is larger than expected and may reflect orientation problems of the diffusograph. Operator notes indicated that the pyrheliometer was correctly adjusted for solar tracking during the day. The traces generally show no cloud depletion except for a very brief interruption after 1000 hours and some apparent light cloud late in the day. The results indicate that cloud-free periods can be identified from radiometric data.

4.6.2 Comparison of Direct Beam Measurements

The measurement of direct beam irradiance by the pyrheliometer requires frequent operator monitoring of the instruments. A much more convenient determination could be provided by the residual approach using the global and diffuse pyranometer systems. This latter approach would eliminate a significant amount of operator time required for the pyrheliometer.

To examine the feasibility of using the alternative of residual direct beam measurements, a comparison of the radiometric techniques was completed. Figure 14 shows the hourly totalized measurements of residual direct beam values plotted against the hourly totals recorded by the pyrheliometer for 286 cases. A linear regression of residual to measured values is given by the following expression:

$$S_{resid} = 142\ [\pm\ 21] + 1.054\ [\pm\ 0.02] * S_{pyrh} \qquad (5.8)$$

where S_{resid} and S_{pyrh} are the residual determined and pyrheliometer measured direct beam irradiance values respectively. The correlation coefficient is 0.95 and the standard error values for the terms are also indicated. Included on the graph is the 1:1 line indicative of perfect agreement and the 20% error bars.

The graph shows similar relationships but the residual values are consistently higher than the measured pyrheliometer values. Indeed, the majority of residual values are greater than the +20% bar with numerous values exceeding 50% error. This overestimation of residual values implies that either the pyrheliometer values were too low or that global and diffuse values were incorrect.

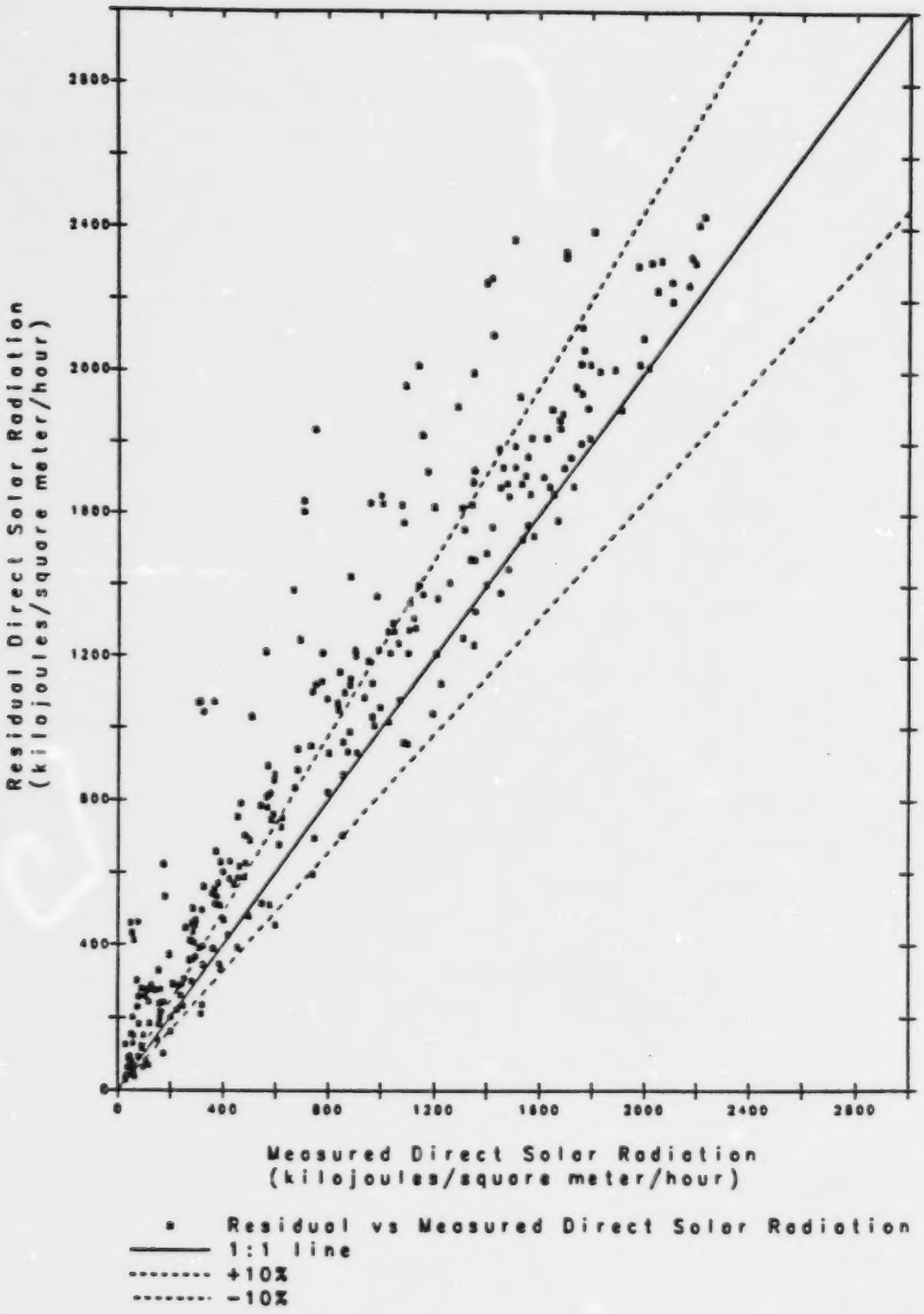

Figure 14. Comparison of Pyrheliometer Measured and Residually Derived Direct Beam Irradiance values (n=286). Indicated are the 1:1 line and 10% error lines.

Given the simplicity of the latter two systems, it appears that a substantial portion of the difference may be attributable to errors in the pyrheliometer measurements. The lower-than-expected pyrheliometer values suggest that slight errors in instrument position caused it not to be centrally focused on the solar disc. In addition, there were times when the signal cable attachment was found wrapped across a portion of the sensing element. Monitoring by the ARC staff documented the need for frequent alignment and cable adjustment. Both of these problems would cause an underestimation of the direct beam intensity. However, with monitoring, accurate values were obtained. The comparison test shows that careful monitoring of the pyrheliometer is required for accurate measurements.

4.6.3 Calculated Aerosol Optical Depths

The lack of AES defined "cloud-free" hours throughout the study period restricted the number of case studies available for sample analysis. Aerosol optical depths were calculated for one day when pyrheliometer operation was closely monitored and identified as being accurate. Aerosol values were calculated by using Equation 5.4 and determining the modelled values of irradiance using the procedures summarized in section 5.3. Tests using both the pyrheliometer-measured direct beam values and those determined by residual techniques were also conducted.

The selected day for aerosol calculations was April 7. Figure 15 graphs the calculated aerosol optical depths calculated for hourly periods of clear sky irradiance for this date. Included on the graph are the hourly aerosol optical depths calculated using the direct pyrheliometer measurements (*) and those calculated by the global-diffuse residual values (+). Values are plotted for the averaged value for the previous elapsed hour.

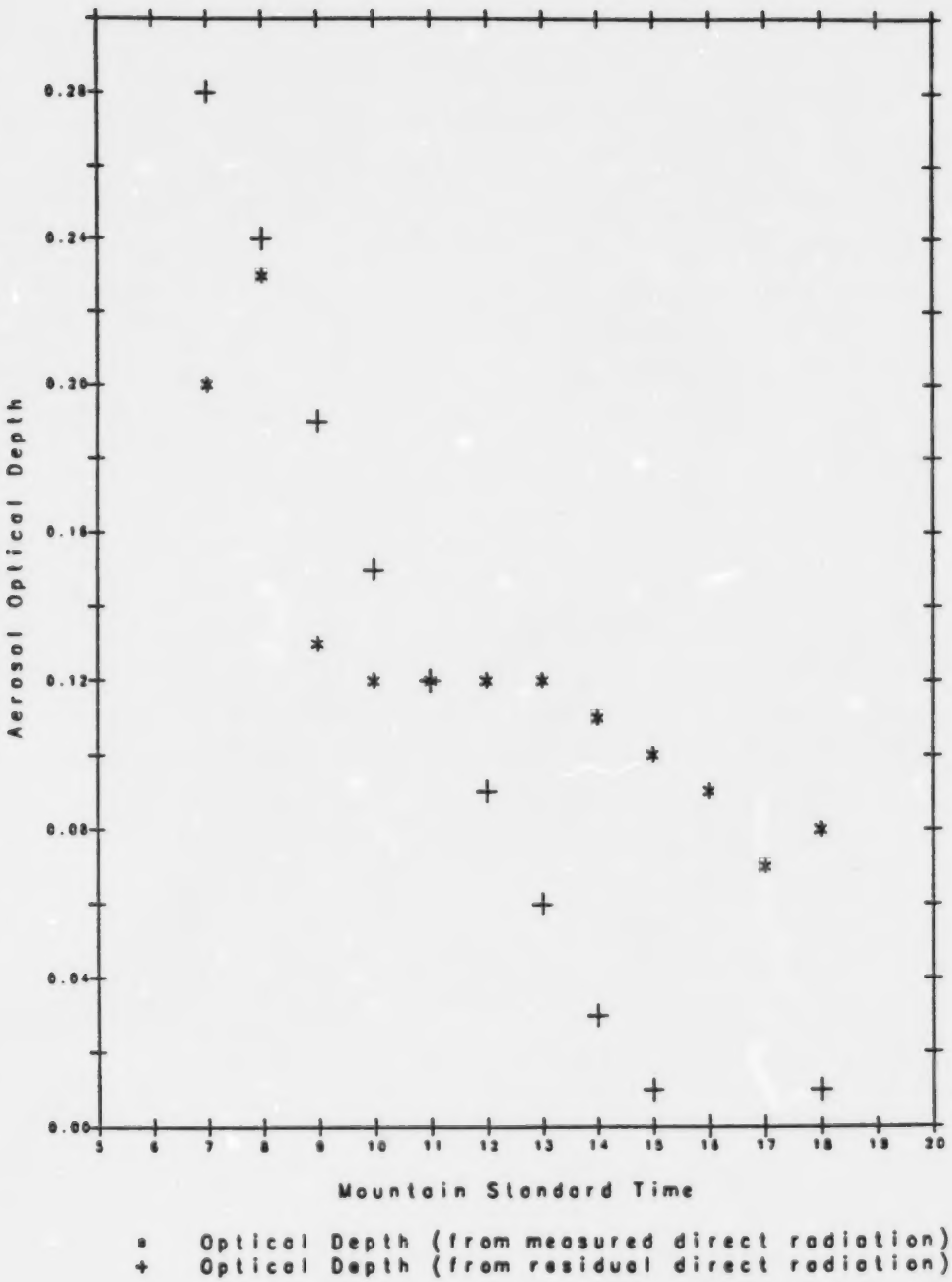

Figure 15. Calculated Hourly Aerosol Optical Depths (ta) for April 7, 1986.

The pyrheliometer values indicate early morning values of 0.20 to 0.23 with a rapid decline to values of about 0.12 by 0900 hours. A decline in aerosol turbidity is exhibited for the remaining daylight hours towards a value of 0.09 at 1800 hours, close to sunset. A minimum τ_a value of 0.08 is calculated at 1700 hours, but actually represents the effects of a few minutes of cloud attenuation suggested by the radiation curve. These values of approximately 0.10 are consistent with reported measurements of turbidity in other Canadian locations (Uboegbulam and Davies, 1983). The higher morning values would be expected due to the higher relative humidities reported in the early hours.

In contrast, the values calculated from the residual direct beam value do not follow the pyrheliometer derived values very well. The graph shows similar high values in the early hours (0.28 to 0.24) but then shows a rapid decline that reaches zero by late afternoon. These results are unexpected and cannot be readily explained. Examination of residual values calculated for the preceding day (April 6) showed a similar pattern. The differences appear to reflect an error in measurement and it is suggested that the diffusograph may have been incorrectly adjusted. The irradiance curves for April 7 show a relatively large difference between the pyrheliometer and residual direct beam values that is accentuated in the afternoon. This suggests that the residual values may be erroneous and would then yield incorrect estimates of the aerosol optical depths.

4.6.4 Radiative Responses to Aerosol Optical Depths

One of the future objectives of the study is to examine the possible climatic effects of the aerosols on the regional climate of Calgary. This effect is postulated to result from changes in the irradiance regime caused by the aerosol layer. While explicit examination of these potential effects is beyond the scope of Phase I of this study, a sample examination of possible responses was made.

The possible radiative response to the aerosols on April 7 was examined by plotting the hourly totals of global and net irradiance values against derived hourly aerosol optical depths. Figure 16 shows the values with both the net and global values normalized by the incident extra-terrestrial irradiance values. The plots show that both the global and the net generally track together, as expected due to the dominance of the global term during daylight hours. There is some indication that net irradiance shows a small increase with increasing aerosol values (up to 0.12) and then follows the global values in a decrease. This very limited data set precludes any general conclusions but illustrates a technique for examining possible responses.

4.6.5 Aerosol Optical Depths and Meteorological Conditions

The sample set of aerosol optical depth measurements precludes any comprehensive comparison with reported visibility and wind measurements. For the April 7 case, the winds were consistently from the west at 5 to 8 m/s throughout the daylight hours. Reported visibility ranges, from the adjacent Calgary Airport AES weather office, ranged from about 25 km in the early hours and then rapidly increased to about 65 km before noon. The meteorological conditions suggested a well-mixed boundary layer that was supported by the afternoon radiosonde profile recorded at Edmonton (the closest to Calgary available). The morning optical depth maximum followed by the decrease to the 0.10 level is consistent with the rapid change in reported visibilities.

Recent studies in the mid-Atlantic region of the US (Peterson and Fee, 1981) showed that horizontal visibility could be related to vertical turbidity by an expression similar to the Koschmieder expression (Equation 1.2). Their results indicated that turbidity measurements explain over 66% of the visibility variation during the summer months. The best results were achieved when

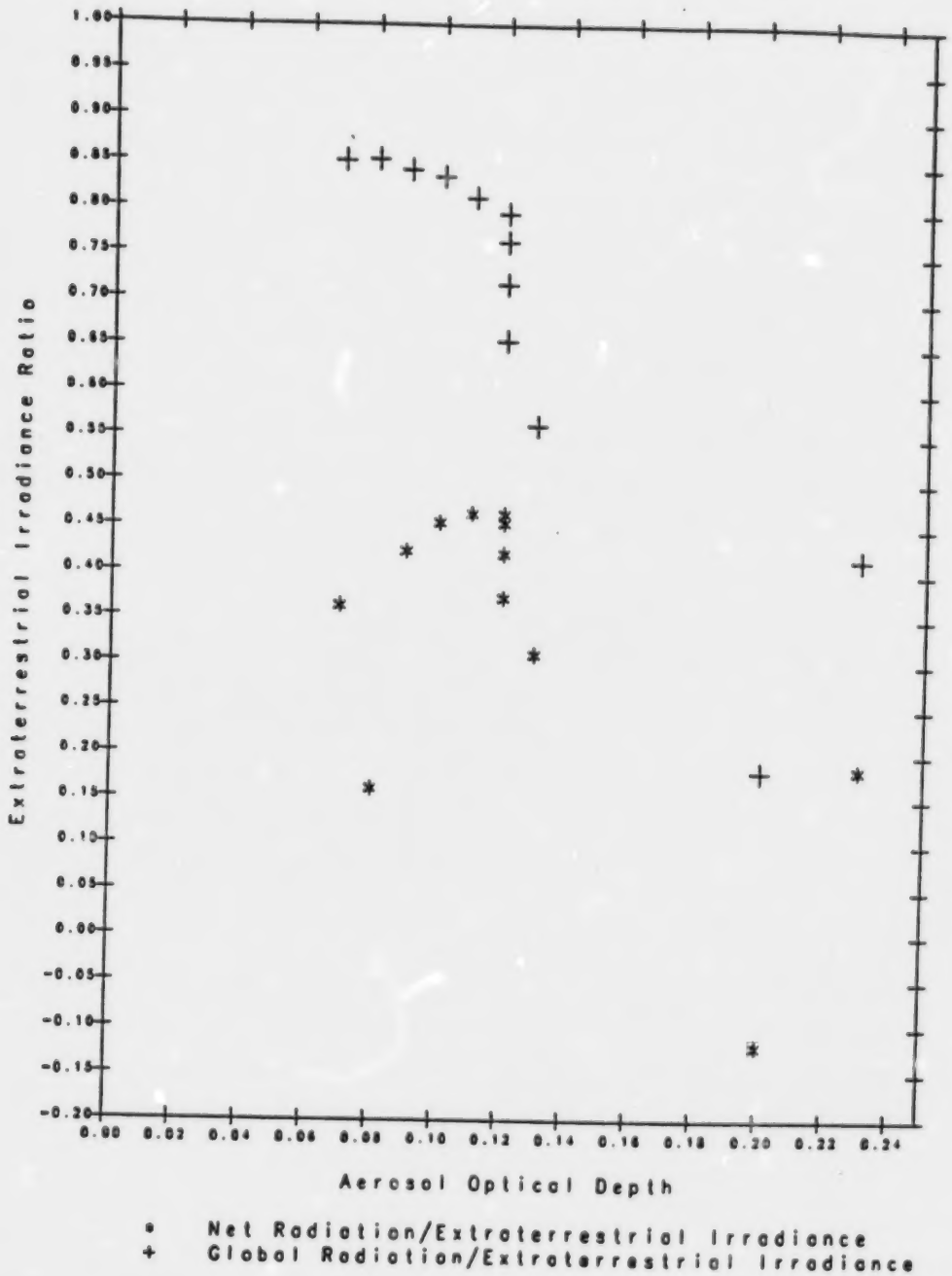

Figure 16. Radiative Response to Aerosol Optical Depths for April 7, 1986. Global (+) and Net (*) values are Normalized by Incident Extraterrestrial Flux.

turbidity measurements were low. The derivation of such a relationship for the Calgary region would be useful for using solar radiometric data for estimating the visual range.

4.6.6 Spectral Measurement Results

Selected spectral irradiance measurements were made on April 8 and 9. This section will note the results made on the latter date when the full measurement program was completed.

The aerosol optical depths for four selected spectral bands identified in Table 3 were calculated using the procedures outlined in Section 4. Values were determined using a series of two-minute averages for the period initiated at 1050 hours on April 9 and extending for approximately one hour. Model values of average irradiance were calculated for the appropriate time period using Equation 5.5 with an assumed ozone concentration of 0.40 atmo-cm. and the atmospheric pressure values from the nearest hourly reading at the Calgary Airport AES weather office.

The values for the spectral bands are plotted in Figure 17 as a log-log plot. The slope of the line can be interpreted as the wavelength exponent, sometimes called the Angstrom turbidity factor (α). It measures the degree of decrease in attenuation with increasing wavelength expressed as follows:

$$b_{ext} = \text{coeff} * \lambda^{-\alpha} \qquad (5.9)$$

The results of the spectral measurements, using the spectral aerosol optical depth as the expression for b_{ext}, give a value of 0.013 for coeff and an α value of 4.51. This indicates a strong wavelength dependence for aerosol attenuation. The limited data of this test

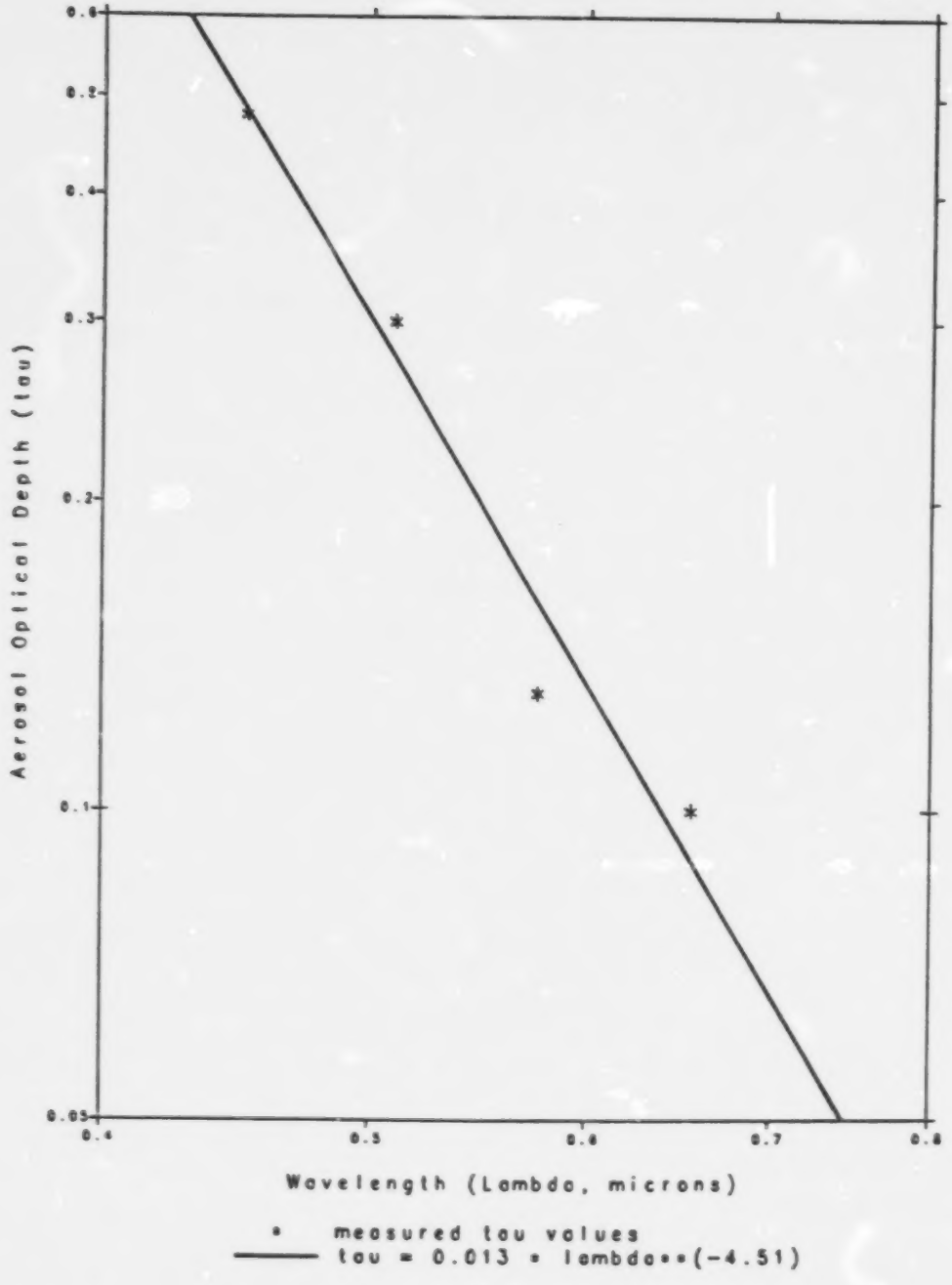

Figure 17. Measured Spectral Aerosol Optical Depths for April 9, 1986. Averaged values for four narrow wavebands are plotted (and the calculated "best-fit" line is ta = 0.013 * l exp(-4.51).

sample restrict discussion, but the strong slope of attenuation would be consistent with an urban atmosphere with a higher number of carbonaceous aerosols characterised by smaller particles (Paltridge and Platt, 1976).

4.7 SUMMARY AND CONCLUSIONS OF RADIATION MEASUREMENT PROGRAM

The program developed and tested procedures for applying radiometric techniques for monitoring the urban aerosol. The following results were achieved with the accompanying conclusions.

(1) A field measurement program was completed and radiation instrumentation tested from February 18 through April 8, 1986 in Calgary. The program indicated that measurements could be made of the components required for aerosol determination, but that frequent operator attention was required for the pyrheliometer. Interpretation of measurements required a monitoring of sensor status.

(2) Components of the radiation regime at Calgary were measured continuously and were presented. These measurements included direct beam, diffuse beam and global solar radiation. In addition, net radiation values were recorded and presented for selected days. The values indicated that, even with frequent cloud cover, periods of clear sky conditions could be identified from the data.

(3) Solar irradiance models for estimating the direct beam solar irradiance were developed and tested.

(4) Pyrheliometer measurements of direct beam irradiance were compared with estimates of direct values derived from the residual between global and diffuse measurements. Pyrheliometer values were frequently underestimated when compared to the residual values. Some of the differences were thought to result from errors in sensor orientation.

(5) Example aerosol optical depths were calculated for a one-day case study (April 7). Optical depths were derived by using modelled values for an aerosol-free atmosphere with measured values. Both pyrheliometer and residual-derived direct beam values were tested. The pyrheliometer-derived values ranged from 0.25 in the early morning with a common value of around 0.10 reached around noon for the rest of the day. These values are consistent with values reported in the literature. Optical depths, derived from residual solar measurements, did not agree with the directly measured values on the test date. The error was attributed to diffusograph ring positioning.

(6) No explicit comparisons of aerosol optical depths with reported meteorological visibility ranges were possible due to the limited sample size. The one-day case study aerosol values and trends were qualitatively consistent with reported visibility values.

(7) The radiative changes with aerosol loadings were analyzed for the April 7 case study. Both global and net irradiance values generally tracked together, with possible differences of the net irradiance at low aerosol levels. More detailed measurements would be required for specifying radiative responses to aerosols.

(8) Spectral aerosol optical depths were calculated for a test measurement program conducted on April 9. The values indicated a strong decrease in aerosol optical depth with increasing wavelength.

5. PROPOSED EXPERIMENTAL DESIGN FOR PHASE II

To determine the effect of urban air quality on visibility in the Calgary region, a coordinated study involving all the major components affecting visibility in the city is required. This is due to the unique meteorological, topographic and chemical characteristics that affect the city's air quality. Thus the study proposed here will encompass investigations of the aerosol physical and chemical characteristics and the meteorological conditions in the Calgary region.

The prime objective of Phase I of this study has been to develop and design a detailed, comprehensive research plan which would meet the needs of urban air resources management and could be implemented in Phase II of the study. The goals of the research plan that has been developed are:

1. To characterize and quantify the temporal and spatial variability of the chemical and physical characteristics of the urban aerosol loading (gases and particulates);

2. To determine the relationship between visibility degradation and aerosol loading;

3. To identify what sources contribute to the aerosol loading and the relative impact of each; and

4. To assess the effects of aerosols on the radiation and energy budgets of urban areas.

To satisfy the first objective, a climatological study of visibility in the Calgary region is proposed as well as a surface measurement program at selected urban sites. Surface and airborne measurements of aerosol characteristics and extinction coefficients at selected sites will provide data for the second objective. Size fractionation of the chemical constituents of the aerosols will help to identify the sources of the aerosols and their relative importance. Finally, a radiation measurement program is proposed to assess the effects of aerosols on energy budgets. These various components of the proposed research plan are discussed in the following sections.

5.1 CLIMATOLOGICAL STUDY OF VISIBILITY IN THE CALGARY REGION

A climatological study of existing visibility and related data is proposed. As insufficient data on aerosols precludes a climatological study of their characteristics, the study will focus primarily on reported visibility ranges. The purpose of the study would be to document the general temporal variation of visibility and to determine if any trends are apparent. This would indicate the best time periods for limited measurement programs. This study would involve the analysis of archived Atmospheric Environment Service hourly meteorological data and other available data sources. Data from Calgary and selected "control" stations upwind of the urban area would be examined.

Statistical analyses of these data sets would be conducted to determine the character of visibility-reducing events. Particular emphasis would be placed on the analysis of a variety of scales including: diurnal-mesoscale variations coincident with local emission and relative humidity patterns, synoptic air mass related variations, seasonal periodicities, and possible longer-term secular trends. Analysis would be conducted using a variety of statistical techniques including time series and correlation analyses. All data would be checked to the extent possible and trends and periodicities would be cross checked.

5.2 SURFACE MEASUREMENT PROGRAM

Pollutants are not homogeneously distributed in the vertical or the horizontal. Because of this, sampling by aircraft is proposed to obtain information on the vertical variations in aerosol concentrations. As well, sampling by aircraft can give indications of horizontal variations. However, due to the expense of research aircraft time, a surface measurement program comprising an upwind, downtown and downwind site is proposed to examine the horizontal and temporal variations.

On the average, surface wind in Calgary has a westerly component. Also, the topography in Calgary is somewhat complex. Given these facts, existing monitoring sites operated by Alberta Environment are proposed as convenient, cost-effective, surface site locations. Thus, the following sites, illustrated in Figure 18, are recommended for the surface measurement program:

1. Upwind location: the University of Calgary site operated by Alberta Environment which is located northwest of Calgary.

2. Downtown location: The Calgary downtown monitoring site operated by Alberta Environment. This unit is currently situated on the rooftop of the police station at 4th Street and 6th Avenue SW but will be moved to a new site one block away very shortly.

3. Downwind location: The Calgary industrial monitoring site operated by Alberta Environment. This unit is at ground level located near the site of the old Bonnybrook Meteorological Tower in the SE Calgary industrial area.

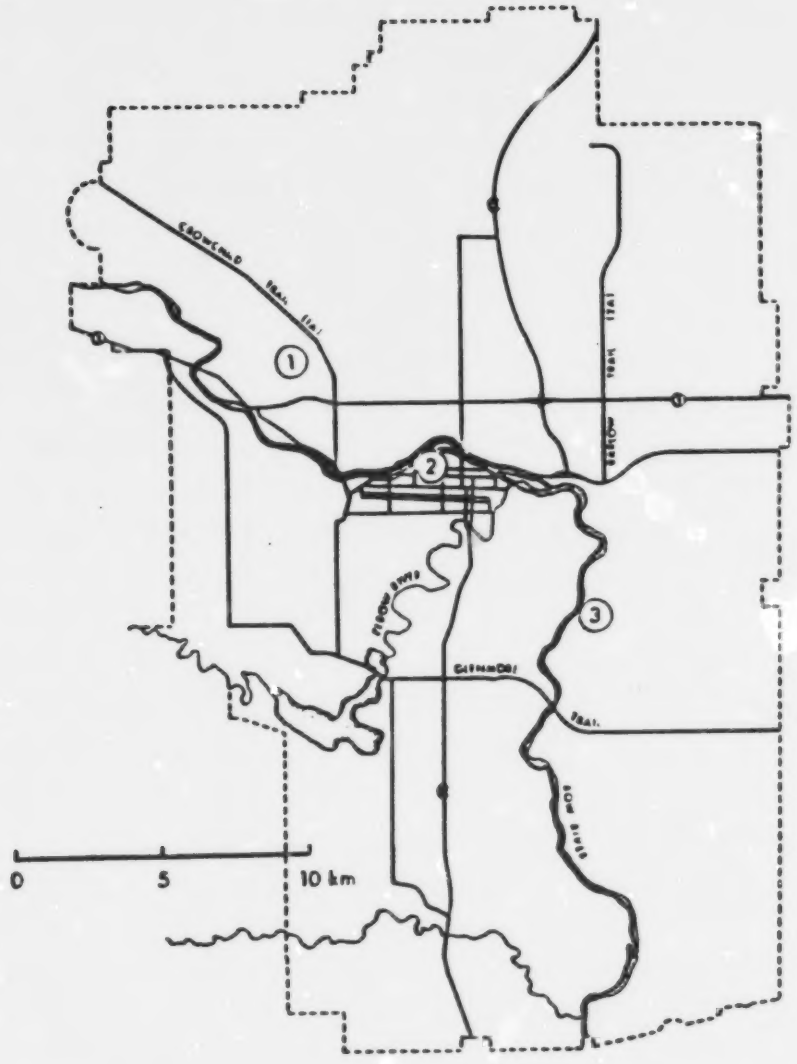

Figure 18. Map of City of Calgary Showing Proposed Location of Observation Sites. (1) Upwind Location: Alberta Environment Residential Monitoring Unit at the University of Calgary; 2) Downtown Location: Alberta Environment Downtown Monitoring Unit; (3) Downwind Location: Alberta Environment Industrial Monitoring Unit.

Actually, it would be desirable for the upwind site to be in more of a rural location, further west than the University of Calgary site. This, however, would involve the establishment of a new sampling site which would increase the cost of the project substantially.

Because of the migration and inhomogeneity of the haze, the shortest feasible frequency of measurement is desired. The KAPS system requires approximately one hour sampling time to provide adequate material for the analysis. Thus, during high pollution days measurements will be taken from 0700 to 1900 every two hours, and during medium pollution days measurements will be made every six hours. Twelve-hour samples will be collected from 1900-0700 daily. On the average, this schedule will provide three types of sampling periods: stable conditions between 0700-1100 hours, transition periods between 1100-1300 hours, and unstable conditions between 1300-1700 hours.

Conduction of the measurement program is proposed for a period of one month during October and November, 1987 for late fall and early winter conditions, and for an additional month during March and April, 1988 for late winter and early spring conditions. These periods are suggested because of the high frequency of occurrence of hazy days as reported by Alberta Environment's Calgary downtown monitoring site, but may be changed if the climatological study of Calgary visibility data suggests other time periods are more appropriate. The components of the measurements are summarized in Table 4 and will be discussed in detail below.

5.2.1 Gaseous Measurements

Nitrogen oxides (NO_x), ozone (O_3), carbon monoxide (CO) and hydrocarbons are measured by the Calgary monitoring units of Alberta Environment for the purpose of pollution control. In addition to the gaseous measurements stated above, sulphur dioxide (SO_2) is measured

TABLE 4. MEASUREMENTS AT THE SELECTED SITES

Parameter	Upwind	Downtown	Downwind	Aircraft
Nitrogen oxides	x	x	x	
Ozone	x	x	x	
Carbon monoxide	x	x	x	
Hydrocarbons	x	x	x	
Sulphur dioxide	x	x	x	
Extinction coefficient		x		
Aerosol size distribution	(x)[a]	x		x
Aerosol chemical composition	x	x	x	x
Temperature	x	x	x	x
Dew point	x	x	x	x
Wind speed	x	x	x	x
Wind direction	x	x	x	x
Irradiance	x	x	x	(x)[b]

[a] If an appropriate instrument is available

[b] If appropriate instrumentation can be mounted on the research aircraft.

at the Calgary Industrial monitoring site. These measurements are valuable in the study of the effect of urban pollutants on visibility. NO_2 can be used to determine the extinction coefficient due to gaseous absorption, b_{ag} in Equation 1.1. The other measurements can be used for the source apportionment of the total extinction coefficient. Ozone is an indicator of photochemical activity. SO_2, NO_x, CO and the hydrocarbons serve as indicators of certain pollution sources such as produced by oil and gas combustion. Additional SO_2 monitors should be located at the University of Calgary and the Calgary downtown monitoring sites for the duration of the measurement periods.

5.2.2 Aerosol Measurements

Aerosol samples are to be collected at the suggested downtown location with a KAPS-impactor system. It would be desirable to have a KAPS-impactor system at all sampling sites, but the potential capital cost likely would preclude this. Therefore, it is proposed that at all three monitoring sites, aerosols are to be collected using a KAPS system attached to a dichotomous sampler. The samples are to be analyzed by x-ray fluorescence spectrometry for the aerosol chemical composition.

The size and concentration of aerosols are to be measured at the Calgary downtown monitoring site by an aerosol probe (PMS ASASP-100 with size range 0.1 to 3.0 um) or an aerosol sampling system (electrical aerosol size analyzer and optical particle counter with size range 0.03 to 0.5 um and 0.3 to 3.0 um, respectively). If an additional aerosol sampling probe is available, it should be installed at the Kananaskis Centre site to obtain upwind aerosol size and concentration information. The particle size distribution and chemical composition provides information about the sources of the aerosols and allows the calculation of the light extinction coefficients due to scattering and absorption by aerosols using Mie scattering theory as demonstrated in Section 3. These procedures should determine the b_{ap}, b_{sp}, and b_{sw} terms identified in Equation 1.1.

5.2.3 Extinction Coefficient Measurement

The total extinction coefficient, b_{ext}, is to be measured at the downtown monitoring site with a telephotometer. This measurement is to be compared to the sum of the individual terms of the extinction coefficient in Equation 1.1 as derived from the gaseous and aerosol measurements discussed above. (It is assumed that b_{sg} remains constant.)

For telephotometer use, a matt black target will be placed at a distance of 10 to 20 m (depending upon the length of the rooftop), with the other measurements located at the midpoint of the path length. Such a close target would provide a better comparison between the extinction coefficient measured by the telephotometer and that calculated from the measurements of gases and aerosols which are essentially point observations.

5.2.4 Meteorological Measurements

Meteorological measurements are to be made at all three monitoring sites to provide a data base for the determination of airflow patterns which determine the movement of the polluted air mass. These measurements comprise temperature, dew point, wind speed and wind direction. These measurements are to be supplemented by the hourly observations recorded at the Calgary International Airport located in northeast Calgary.

5.2.5 Solar Radiation Measurements

Measurements of solar irradiance are to be taken to monitor the variability of the Calgary aerosol optical depth. The preferred method would be narrow-band spectral measurements using a filterwheel approach used in Phase I. The advantages of the filterwheel approach

include: narrow-band data to increase accuracy of optical depth estimates, minimization of circumsolar irradiance effects, avoidance of water-vapour absorption bands and increased number of wavelengths for size distribution calculations. These measurements would require the obtaining of an appropriate filterwheel radiometer. Costs can be minimized through a short-term loan arrangement.

An alternate approach would be to use an Eppley normal incidence pyrheliometer attached to a sun-tracking equatorial mount at the downtown site for measuring direct beam irradiance for the aseosol optical depth determination. Additional co-located radiation instrumentation at all sites would include a pyranometer (total solar), a diffusometer (diffuse solar) and a net radiometer (net terrestrial and solar.) These latter instruments would be used for interpreting radiative responses to aerosol variations. Spectral measurements of the aerosol optical depth are to be made if aircraft measurements are made.

5.3 AIRCRAFT MEASUREMENT PROGRAM

An instrumented aircraft is required to determine the vertical distribution of aerosols. Aircraft measurements could also be used to obtain information about the horizontal ditribution of aerosols. Thus atmospheric state parameters and aerosol size distributions are to be obtained with a suitably instrumented aircraft. As well aerosol samples are to be collected using the aircraft to determine the chemical characteristics of the atmospheric particles. Irradiance measurements are also to be made if appropriate instrumentation can be mounted on the research aircraft. A typical flight plan for the aircraft measurements is shown in Figure 19. However the flight plan is to be flexible and may be revised daily, depending upon the orientation of the haze cloud. The horizontal traverses are to be flown between 50-250 m above ground and the spirals from 50-1000 m above ground. Filter samples are to be taken during the horizontal traverses, but no aerosol sampling can be conducted during vertical spirals because of the relatively long

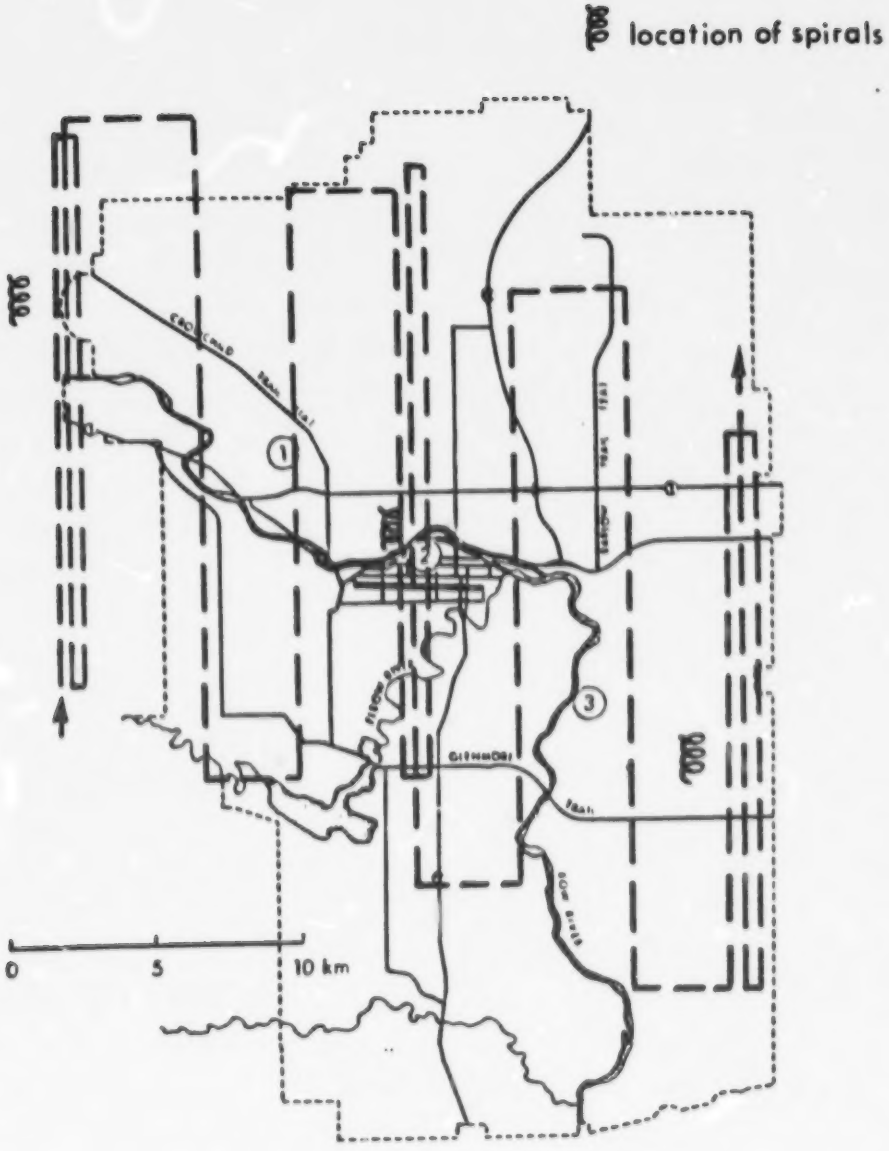

Figure 19. Typical Flight Path for Aircraft Measurement Program. Aerosol Samples Are to Be Collected at the Triple Traverses Closely Outlined in the Diagram. The Same Flight Path Is to Be Repeated at Different Altitude.

sampling time required to obtain representative samples. The aircraft measurements will only be made during day light hours with permission from Transport Canada.

Although it would be desirable to have aircraft measurements throughout each of the proposed measurement periods, the enormous expense of research aircraft time will most likely preclude this. Futhermore, considerable initial outlays of money for instruments such as the telephotometer are required for the project. It is therefore proposed that Phase II of the project be conducted during a period of two fiscal years and that a research aircraft be included in the project only in the second year for only a short time period such as seven to ten days.

5.4 EXPECTED RESULTS

Temporal variations of visibility in Calgary are to be identified. The various terms in Equation 1.1 are to be calculated using the aerosol characteristics and the gaseous measurements obtained at the downtown site. The total extinction coefficient measured with the telephotometer is to be compared to that computed from the other observations. The temporal variations in the visibility reducing species in Calgary are to be determined. Using the chemical measurements at the three sites and the emission data routinely tabulated by Alberta Environment, estimates of the contributions of the various sources to the fine particle mass and the visual range reduction are to be obtained through multivariate analysis. A measurement of atmospheric turbidity of Calgary, as expressed by the aerosol optical depth, is to be derived from radiation measurements and calculated surface irradiance for an aerosol-free atmosphere. Spatial variability of the chemical and physical characteristics of Calgary's aerosol loading and the visibility degradation is to be determined from the aircraft measurements. The effect of aerosols on the atmospheric heating rates is to be derived from the vertical gradients of the radiative flux.

These results should satisfy the needs of urban air resource management and they should be obtainable at a relatively modest cost.

5.6 CONCLUSIONS

A comprehensive research plan has been designed to meet the minimum requirements of urban air resource management.

6. SUMMARY AND CONCLUSIONS

A comprehensive research plan has been developed to study the effect of urban air quality on visibility.

In addition to the development of the plan, considerable instrument and analysis procedure development has been completed and tested in preparation for plan implementation. This has included the development and testing of a KAPS-impactor sampling system. This system will allow the separation and collection of aerosol particles according to size with a minimum of alteration in particle chemical composition. Vertical profiles of aerosol concentration have been derived from data collected by a research aircraft and profiles of extinction coefficients due to aerosol scattering and absorption have been calculated from these profiles and Mie theory. These profiles illustrate the valuable contribution a research aircraft can make in air quality studies. Irradiance instruments have been tested and procedures for calculating aerosol loadings derived. Sample aerosol optical depths were calculated. Spectral optical depths were calculated which indicated a strong decrease in optical depth with increasing wavelength. These measurements indicate the possibility of using solar radiometric techniques for monitoring regional aerosol loading.

The accomplishments of Phase 1 should greatly facilitate the implementation of the proposed research plan for Phase 2. With the experience gained through completion of the development and testing of some of the required instrumentation and analysis procedures, Phase 2 should proceed with little difficulty.

7. REFERENCES

Barlow, F. D., 1979: Modelling solar radiation components in aerosol atmospheres, M.Sc. Thesis, McMaster University, Hamilton, Ontario, pp. xii, 128.

Bohren, C. F., 1983: Absorption and scattering of light by small particles. John Wiley and Sons, New York, 530pp.

Buma, T. J., 1960: A statistical study of the relationship between visibility and relative humidity at Leeuwarden. Bull. Amer. Meteor. Soc., 41, 357-360.

Cheng, L., E. Peake, D. Rogers, A. Davis, 1986: Oxidation of nitric oxide controlled by turbulent mixing in plumes from an oil sands extraction plant, Atmos. Environ. (in press).

Davies, J. A. and J. E. Hay, 1980: Calculation of the solar radiation incident on a horizontal surface, Proceedings of First Canadian Solar Radiation Data Workshop, April (1978), J. E. Hay and T. K. Won (eds.), Ministry of Supply and Services, Canada.

Davies, J. A. and K. Stewart, 1984: The relationship between turbidity and spectral optical depth, Atmosphere-Ocean, 22, 256-260.

Dutsch, H.U., 1969: Atmospheric ozone and ultraviolet radiation. Climate of the Free Atmosphere., Vol. 4, World Survey of Climatology, (D.F. Rex, ed.), Elsevier, New York, 383-430.

Elterman, L., 1968: U.V., Visible and I.R. Attenuation for atmospheres to 50 km. Environmental Research Papers, No. 285, AFCRL-68-0153, Bedford, Mass.

Freund, J., 1983: Aerosol optical depth in the Canadian Arctic, Atmosphere-Ocean, 21, 158-167.

Groblicki, P. J., G. T. Wolff and R. J. Countess, 1981: Visibility-reducing species in the Denver "brown cloud" - I. Relationships between extinction and chemical composition. Atmospheric Environment, 15, 2473-2484.

Harrison, A. W. and C. V. Mathai, 1980: Particulate air pollution and visibility over Calgary. Prep. for Research Secretariat, Alberta Environment by Physics Department, University of Calgary. RMD-80/2. 99 pp.

Hickey, J.R., L.L. Stowe, H. Jacobwitz, P. Pellegrino, R.H. Maschoff, F. House and T.H. VonderHarr, 1980: Initial solar irradiance determinations from Nimbus 7 cavity radiometer measurements. Science, 208, 281-283.

Isaac, G. A., W. R. Leaitch, J. W. Strapp and K. G. Anlauf, 1985: Summer aerosol profiles over Algonquin Park, Canada. Submitted to Atmospheric Environment.

Kasten, F., 1966: A new table and approximate formula for the relative optical air mass. Arch. Meteor. Geophys. Bioklimatol., Ser. B, 14, 206-223.

Kerker, M. (1969): The scattering of light and other electromagnetic radiation. Academic Press, New York, 666 pp.

Lacis, A.A. and J.E. Hansen, 1974: A parameterization for the absorption of solar radiation in the Earth's atmosphere. J. Atmos. Sci., 31, 118-133.

Latimer, J.R., 1972: Radiation Measurement, Technical Manual No. 2, International Field Year for the Great Lakes, Atmospheric Environment Service, Environment Canada.

Leaderer, B. P., R. L. Tanner, P. J. Lioy and J. A. J. Stolwijk, 1981: Seasonal variations in light scattering in the New York region and their relation to sources. Atmospheric Environment, 15, 2407-2420.

Lyons, T. J. and D. R. Cutten, 1975: Atmospheric pollutant and temperature traverses in an urban area. Atmospheric Environment, 9, 731-737.

McCullough, E.C., 1968: Total daily radiant energy available extraterrestrially as a harmonic series of the day of year. Arch. Meteor. Geophys. Bioklimatol., Ser. B, 16, 129-143.

Paltridge, G.W. and C.M.R. Platt, 1976: Radiative processses in meteorology and climatology. Elsevier Sci. Pub. Co., New York, N.Y., 318 pp.

Peake, E., 1980: A preliminary study of the chemical composition of particulate matter and aerosols over Calgary. Prep. for Research Secretariat, Alberta Environment by Kananaskis Centre for Environmental Research, University of Calgary. RS 78-19, 60 pp.

Peterson, J.T. and C.J. Fee, 1981: Visibility-turbidity dependence at Rayleigh, North Carolina, Atmospheric Environment, 15, 2561-2563.

Possanzini, M.A., A. Febo, A. Liberti, 1983: New design of a high performance denuder for the sampling of atmospheric pollutants, Atmos. Eniviron., 17, 2605-2610.

Rodgers, C.D., 1967: The radiative heat budget of the troposphere and lower stratosphere. Report No. A2, Planetary Circulations Project, Dept. Meteor., M.I.T., 99 pp.

Sandhu, H.S., 1975: A study of photochemical air pollutants in the urban airsheds of Edmonton and Calgary, Staff Report 1, Research Secretariat, Alberta Department of the Environment, 155 pp.

Thekaekara, M.P., 1973: Solar energy outside the Earth's atmosphere, Solar Energy, 14, 109-127.

Uboegbulam, T. C. and J. A. Davis, 1983: Turbidity in Eastern Canada, J. Clim. Appl. Meteorol., 22, 1384-1392.

Unsworth, M. H. and J. L. Monteith, 1972: Aerosol and solar radiation in Britain, Q.J.R. Meteorl Soc. 98, 778-797.

Waggoner, A.P. and R.J. Charlson, 1977: Measurement of aerosol optical properties. In Denver Air Pollution Study, 1973, Vo. II, EPA-600/9-770-001, Research Triangle Park, NC, 35-56.

White, W. H. and P. T. Roberts, 1977: On the nature and origins of visibility-reducing aerosols in the Los Angeles air basin. Atmos. Environ., 11, 803-812.

Wolff, G. T., R. J. Countess, P. J. Groblicki, M. A. Ferman, S. H. Cadle and J. L. Muhlbaier, 1980: Visibility-reducing species in the Denver "brown cloud" - II. Sources and temporal patterns. Atmos. Environ., 15, 2485-2502.

Yamamoto, G., 1962: Direct absorption of solar radiation by atmospheric water vapour, carbon dioxide and molecular oxygen, J. Atmos. Sci., 19, 182-188.

8. APPENDIX

Figures A.1 through A.8 present the hourly intergrated solar irradiance values recorded during the field program from March 1, 1986 to April 8, 1986 inclusive. Plotted are global, direct beam measured by the pyrheliometer, direct beam is derived residually, and diffuse. The direct beam values are expressed both as those values measured explicitly by the pyrheliometer and as the residual of the global minus the diffuse. For presentation simplicity, net irradiance values are not considered of primary importance and are not plotted.

The plots indicate the variable nature of the radiation regime. Some days (e.g., March 8 and 19) show near symmetry of the components around noon while other days (e.g., March 17 and 24) show a highly variable regime. These changes are due principally to changing cloud conditions and are indentifiable by those periods when direct beam values are strongly attenuated. Frequently coincident with the direct attenuation is an increase in the relative contribution of the diffuse irradiance characteristic of cloudy conditions. On some days (e.g., March 7 and 9) almost the entire global irradiance is composed of diffuse values only, indicating heavy and persistent overcast cloud conditions. Additionally, the graphs show the general trend to increasing irradiance values reflecting the longer day lengths and higher solar elevations accompanying the spring.

The graphs also show some of the measurement problems associated with the use of the instruments. Specifically, the agreement between the measured and residually derived direct beam values show variations indicative of instrument error. On most days both measurements of direct beam appear to agree well and track well together. On some days (e.g., March 20 and April 6) the differences are quite large and identify periods when instrument alignments were off. Inspection of operators notes confirm that these periods of poor agreement coincide with pyrheliometer or diffusograph orientation errors.

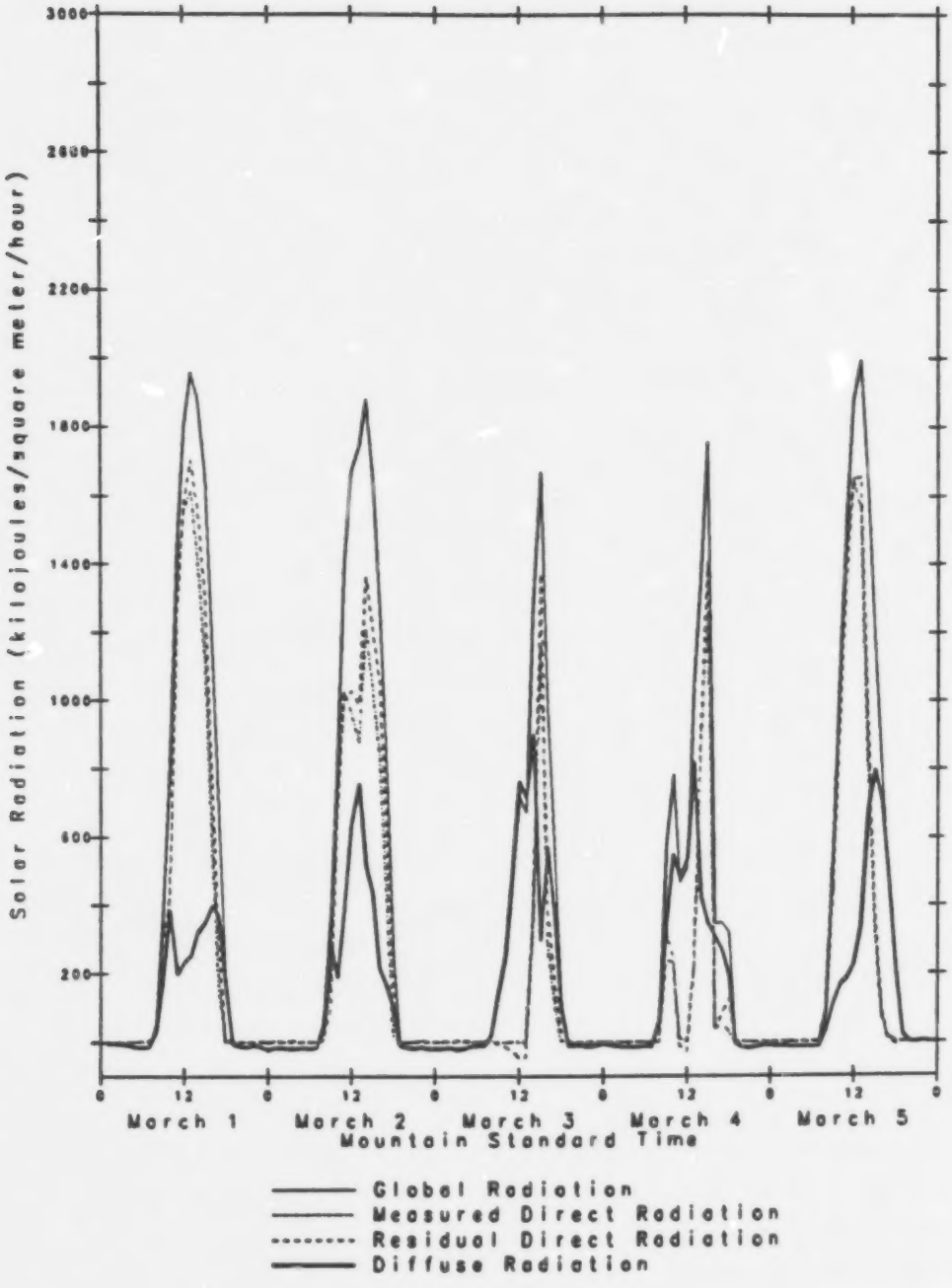

Figure A.1. Measured Solar Radiation Components for March 1 to 5, 1986 (Calgary).

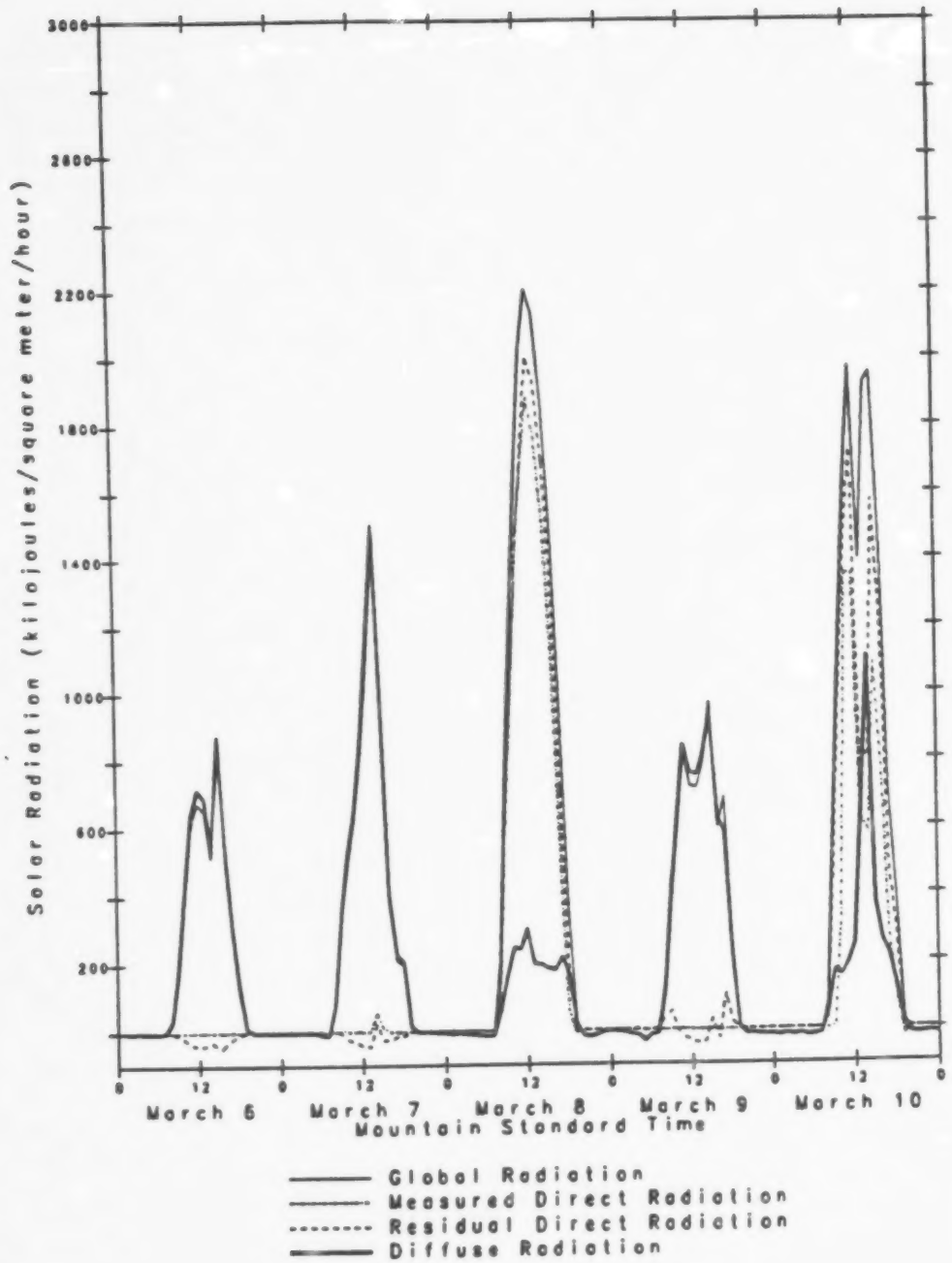

Figure A.2. Measured Solar Radiation Components for March 6 to 10, 1986 (Calgary).

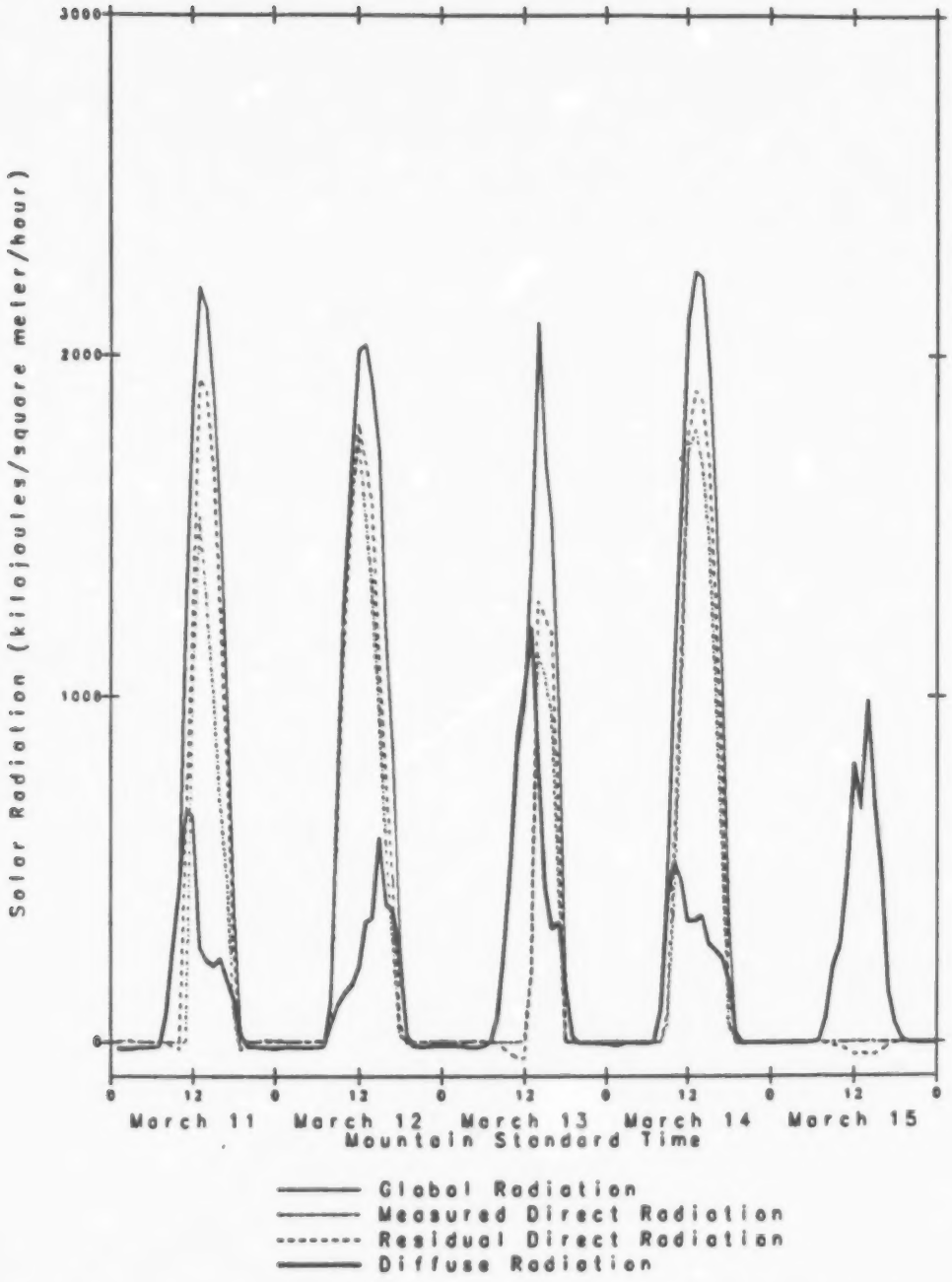

Figure A.3. Measured Solar Radiation Components for March 11 to 15, 1986 (Calgary).

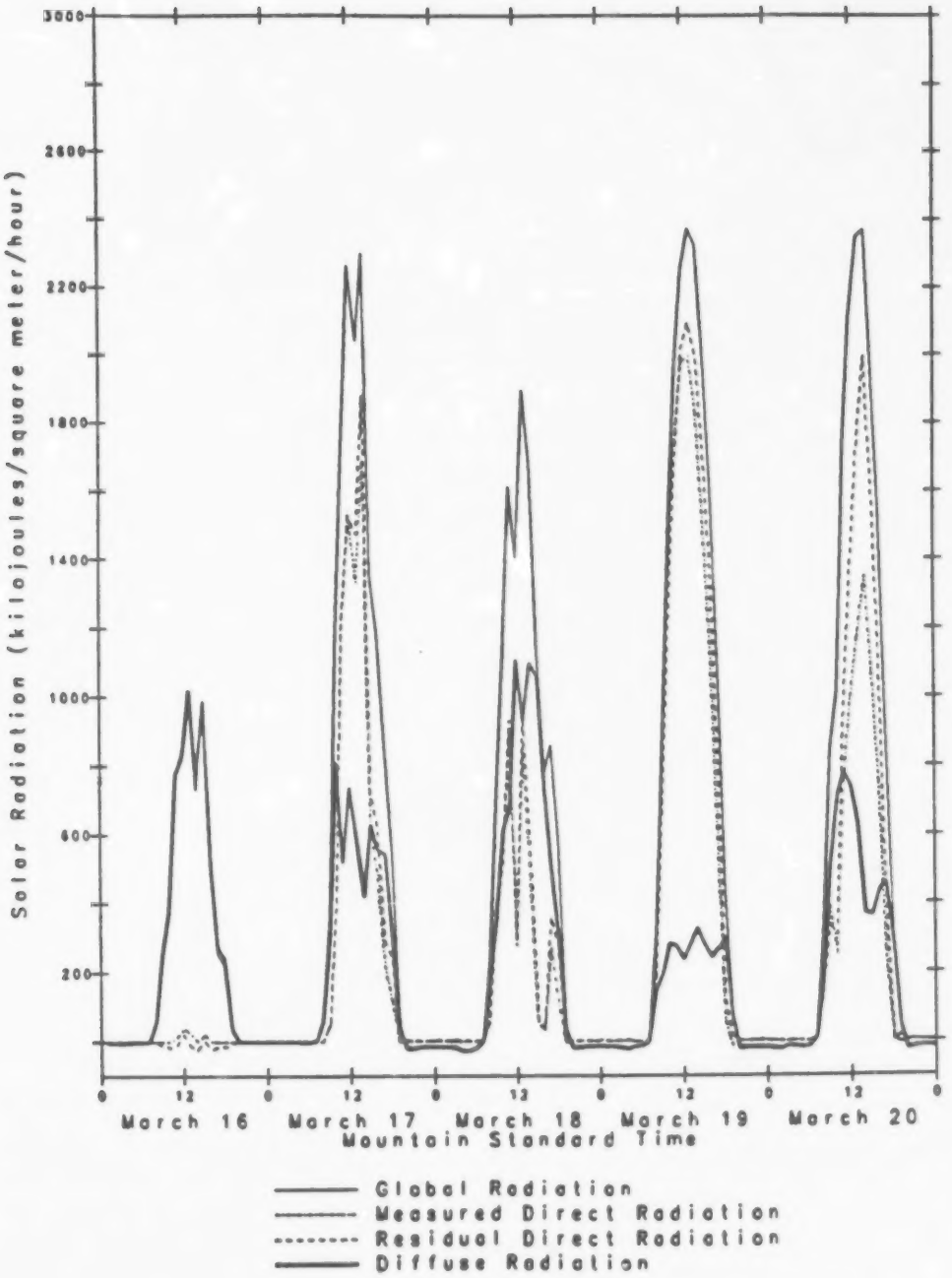

Figure A.4. Measured Solar Radiation Components for March 16 to 20, 1986 (Calgary).

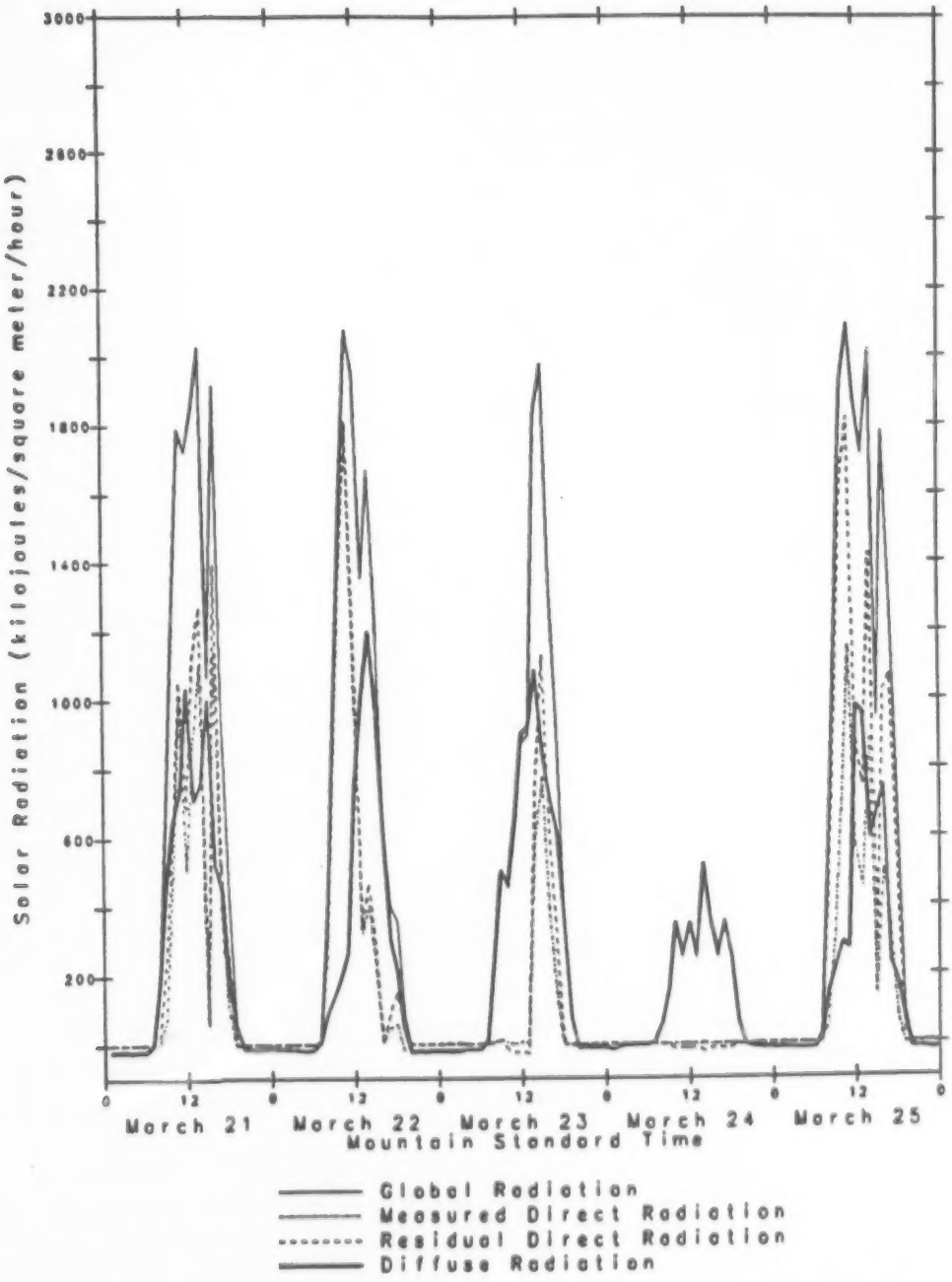

Figure A.5. Measured Solar Radiation Components for March 21 to 25, 1986 (Calgary).

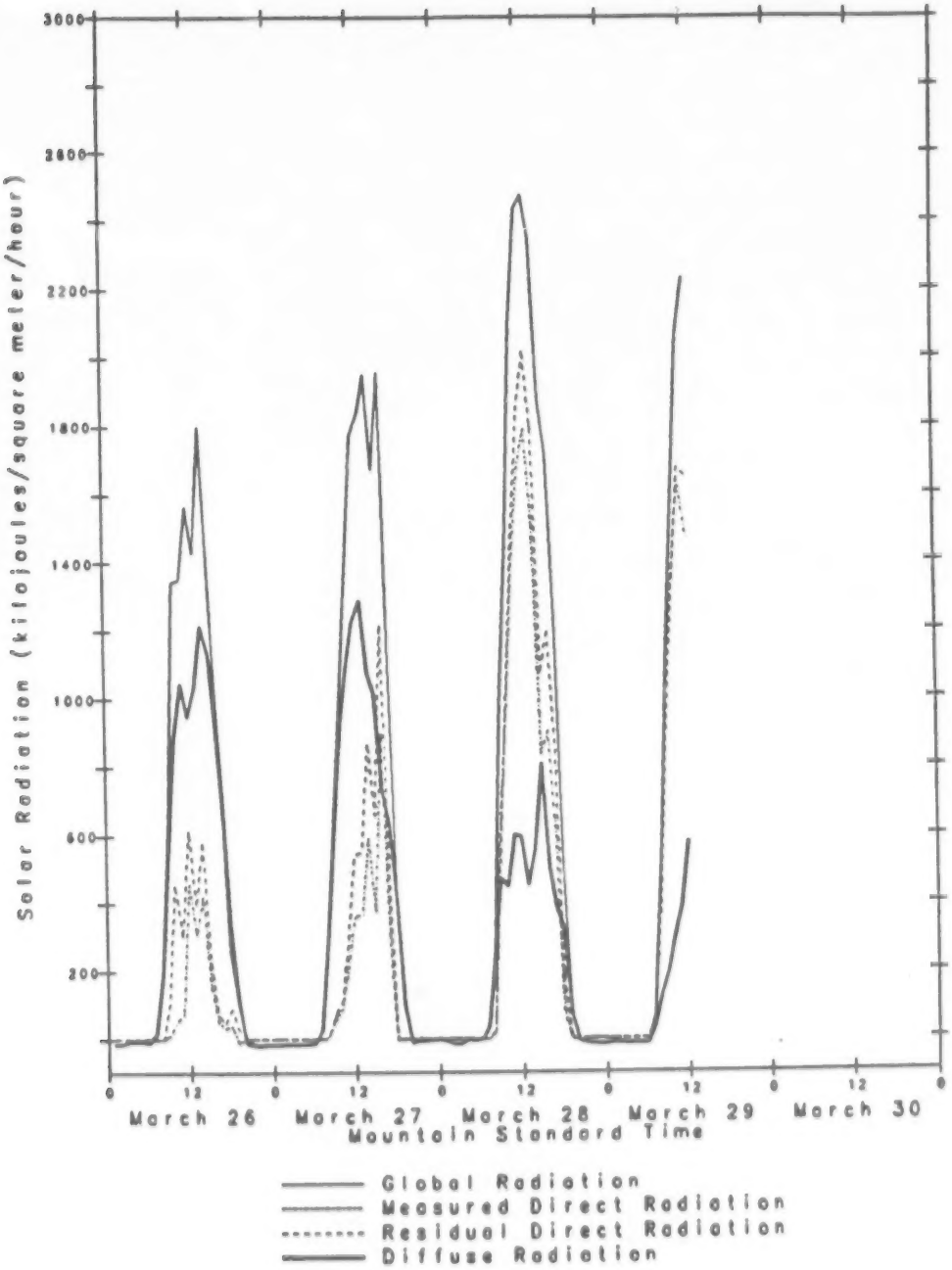

Figure A.6. Measured Solar Radiation Components for March 26 to 30, 1986 (Calgary).

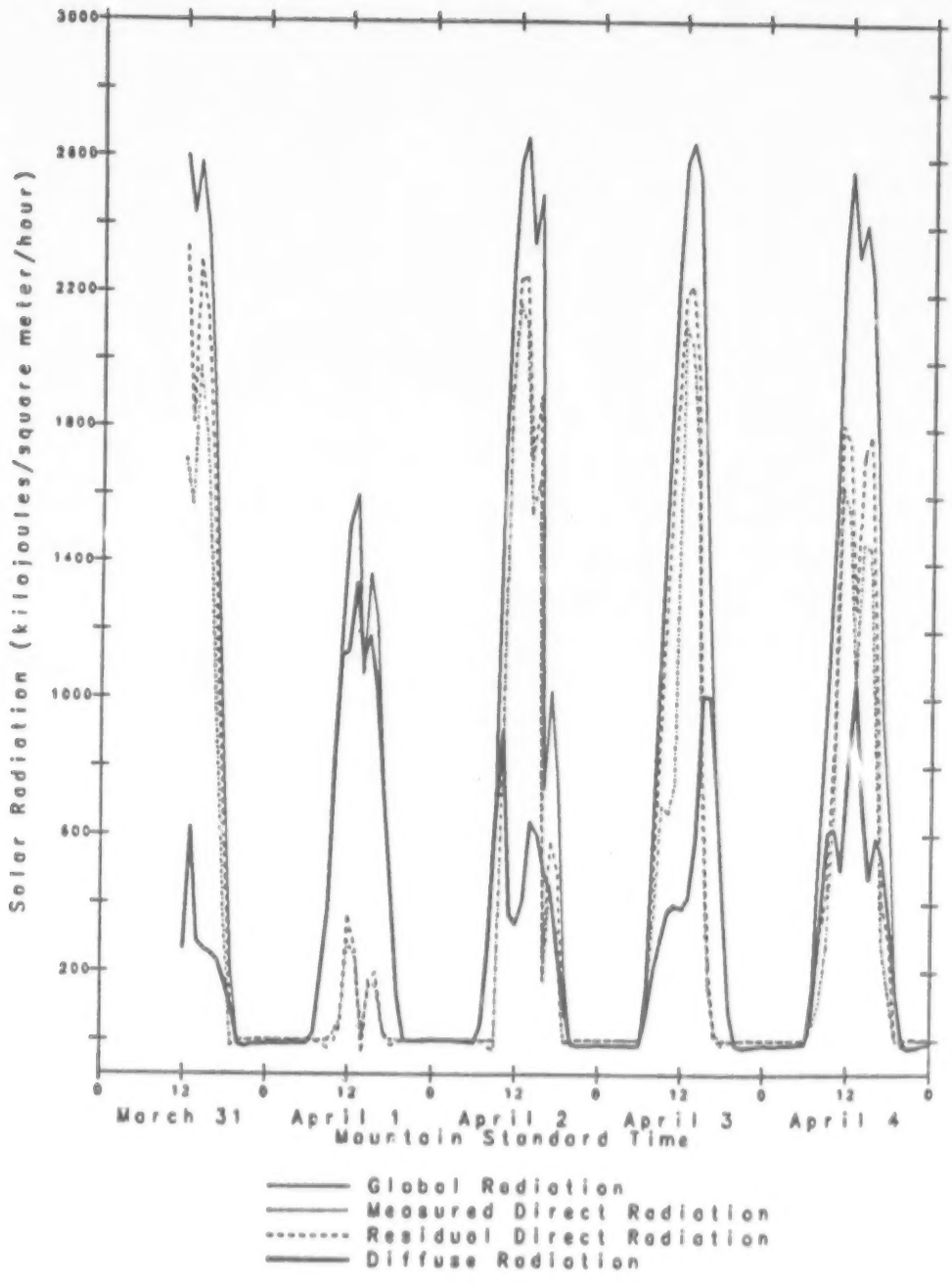

Figure A.7. Measured Solar Radiation Components for March 31 to April 4, 1986 (Calgary).

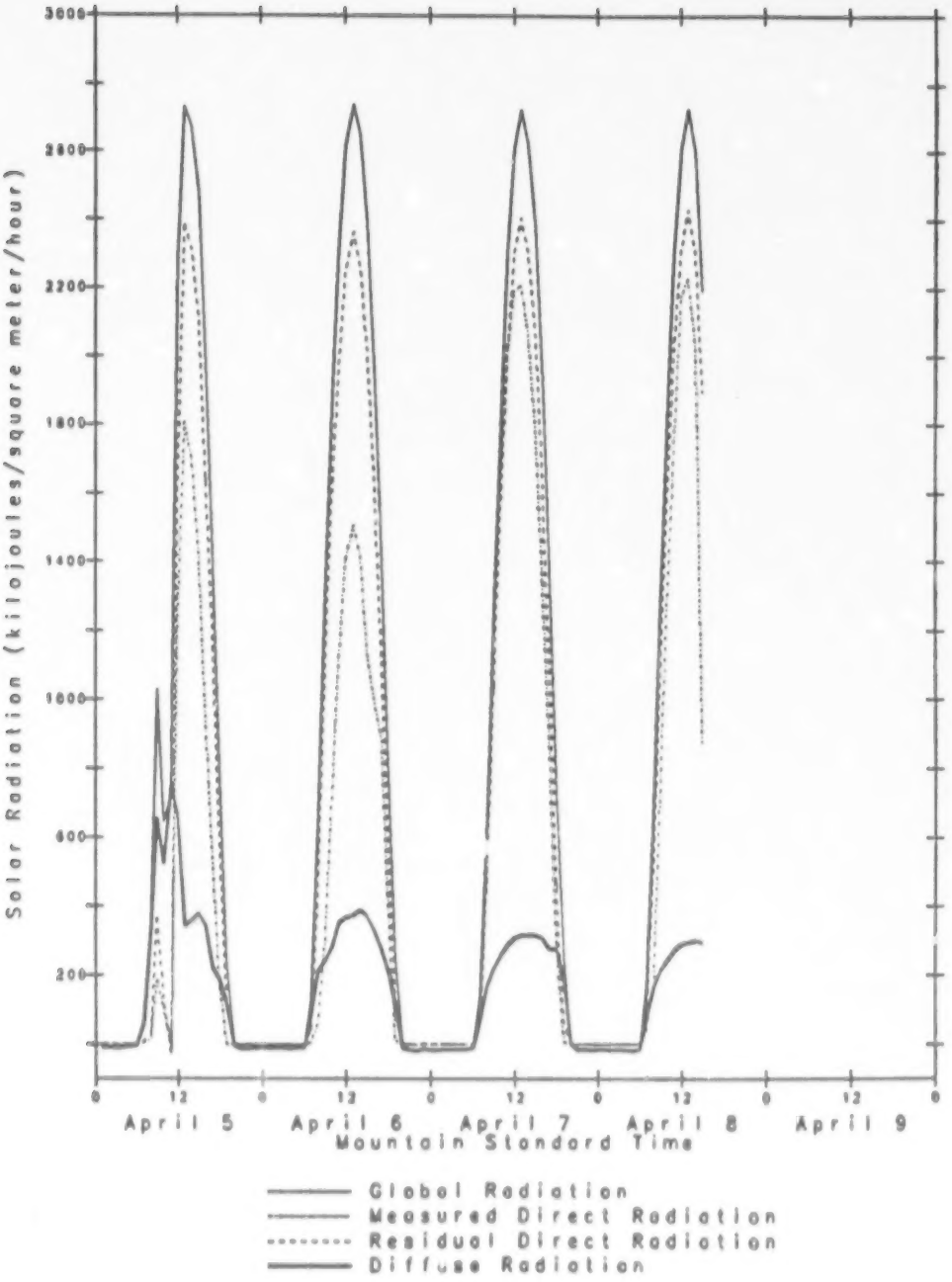

Figure A.8. Measured Solar Radiation Components for April 5 to 9, 1986 (Calgary).